Jet Tomography in High Energy Heavy-Ion Collisions

Yayun He
South China Normal University
South China University of Technology

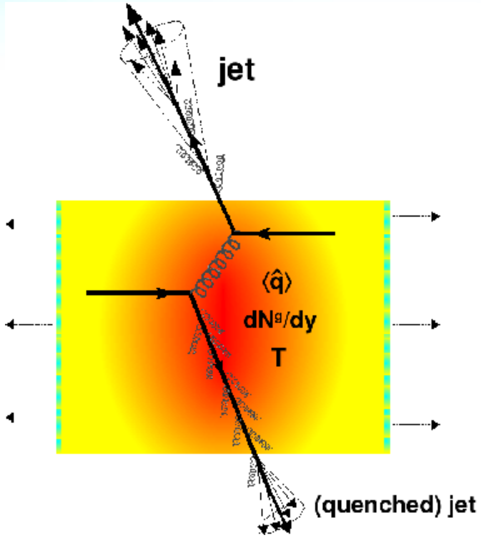

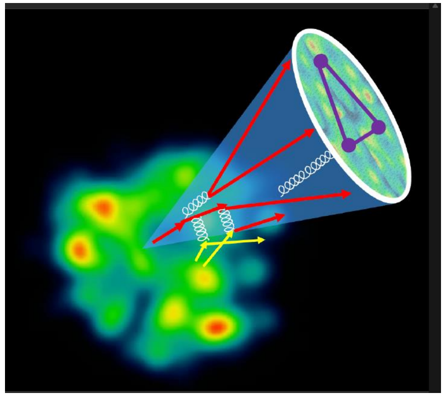

USTC-PNP-Nuclear Physics Mini Workshop Series
Hefei, 2024-06-16

Jet Production in HIC

Jet: hard probe, perturbatively calculable, multiple scales ranging from 1 GeV to 1 TeV

Within the factorized parton model in pQCD,

$$\frac{d\sigma_{AA}^{jet}}{dp_T d\eta} = N_{bin}(b) \sum_{a,b,c} \int d\Delta p_T W_{AA}^{c}(\Delta p_T, p_T + \Delta p_T, R)$$

$$\times f_{a/A} \otimes f_{b/A} \otimes H_{ab}^{c} \otimes J_c(p_T + \Delta p_T, R | p_{T,c})$$

J_c: jet function in vacuum, describe the probability to form a jet from parton c

Kang, Ringer, and Vitev, JHEP 10 (2016) 125

Kang, Ringer, and Vitev, PLB 769, 242 (2017)

W_{AA}^{c}: jet energy loss distribution averaged over initial production points, propagation directions

He, Pang, and Wang, PRL 122, 252302 (2019)

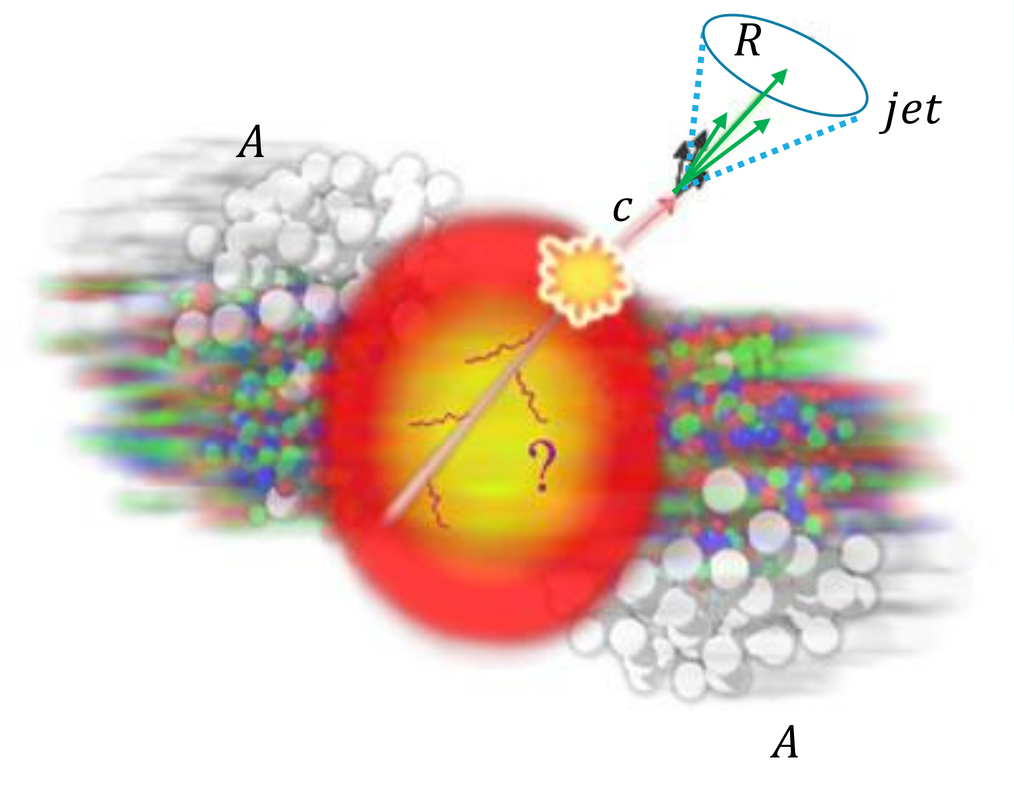

A Sketch of HIC, from lbl website

Jet quenching: energy loss + transverse momentum broadening

Jet Observables in HIC

Jet nuclear modification factor

$$R_{AA} = \frac{d\sigma^{AA}}{\langle N_{coll} \rangle \, d\sigma^{pp}}$$

- ✓ Strong centrality dependence – jet quenching
- ✓ Weak p_T and colliding energy dependence – competition btw the initial spectrum and jet quenching

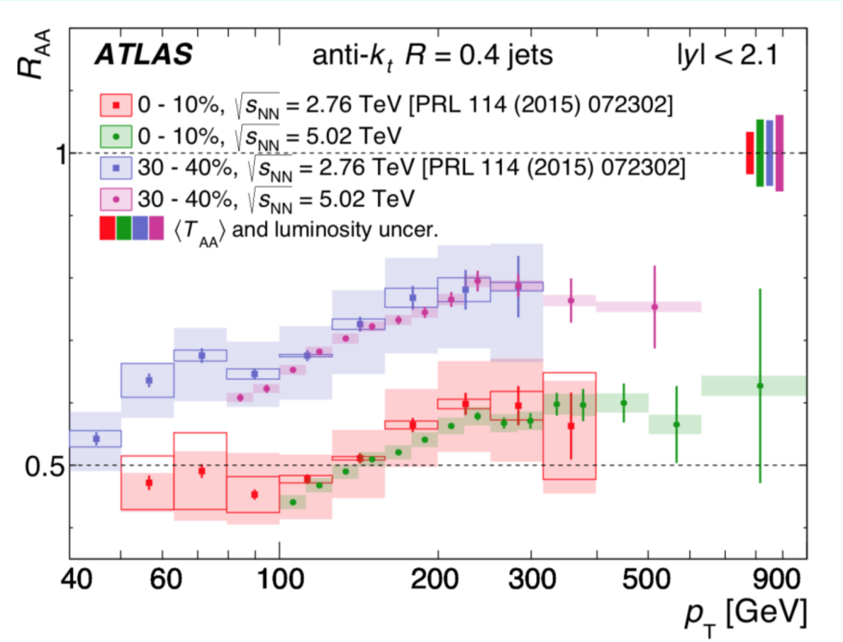

ATLAS Collaboration, PRL 114, 072302 (2015)
ATLAS Collaboration, PLB 790 , 108 (2019)

Jet Observables in HIC

Jet nuclear modification factor

$$R_{AA} = \frac{d\sigma^{AA}}{\langle N_{coll} \rangle \, d\sigma^{pp}}$$

- ✓ Strong centrality dependence – jet quenching
- ✓ Weak p_T and colliding energy dependence – competition btw the initial spectrum and jet quenching

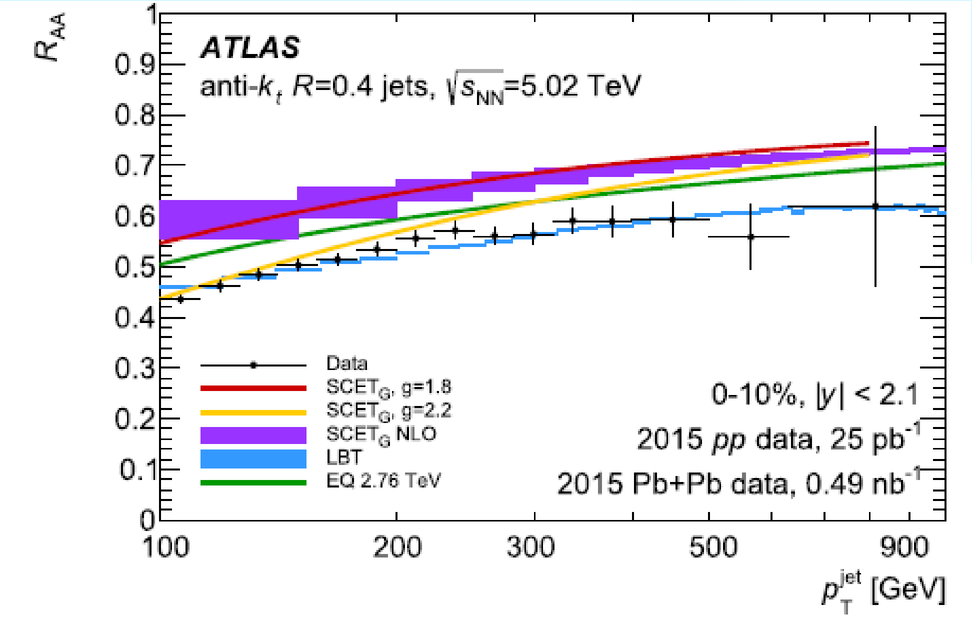

ATLAS Collaboration, PRL 114, 072302 (2015)
ATLAS Collaboration, PLB 790 , 108 (2019)

Jet Observables in HIC

Jet nuclear modification factor

$$R_{AA} = \frac{d\sigma^{AA}}{\langle N_{coll}\rangle \, d\sigma^{pp}}$$

- ✓ Strong centrality dependence – jet quenching
- ✓ Weak p_T and colliding energy dependence – competition btw the initial spectrum and jet quenching
- ✓ R dependence – differential, capable to constrain jet quenching models

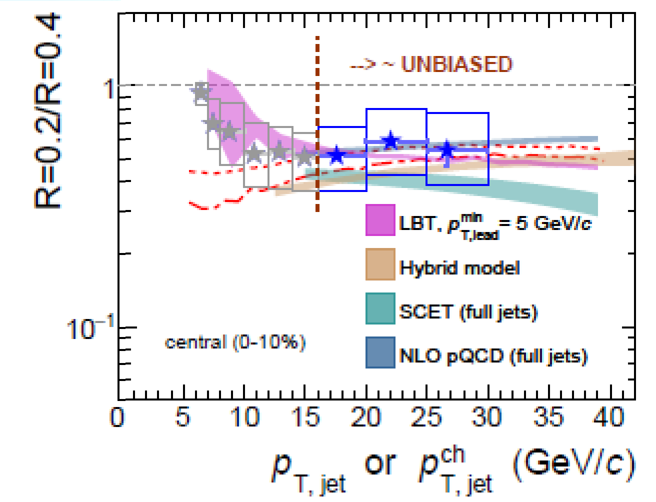

STAR Collaboration, PRC, 102, 054913 (2020)

Jet Observables in HIC

Jet nuclear modification factor

$$R_{AA} = \frac{d\sigma^{AA}}{\langle N_{coll}\rangle \, d\sigma^{pp}}$$

- ✓ Strong centrality dependence – jet quenching
- ✓ Weak p_T and colliding energy dependence – competition btw the initial spectrum and jet quenching
- ✓ R dependence – differential, capable to constrain transport model

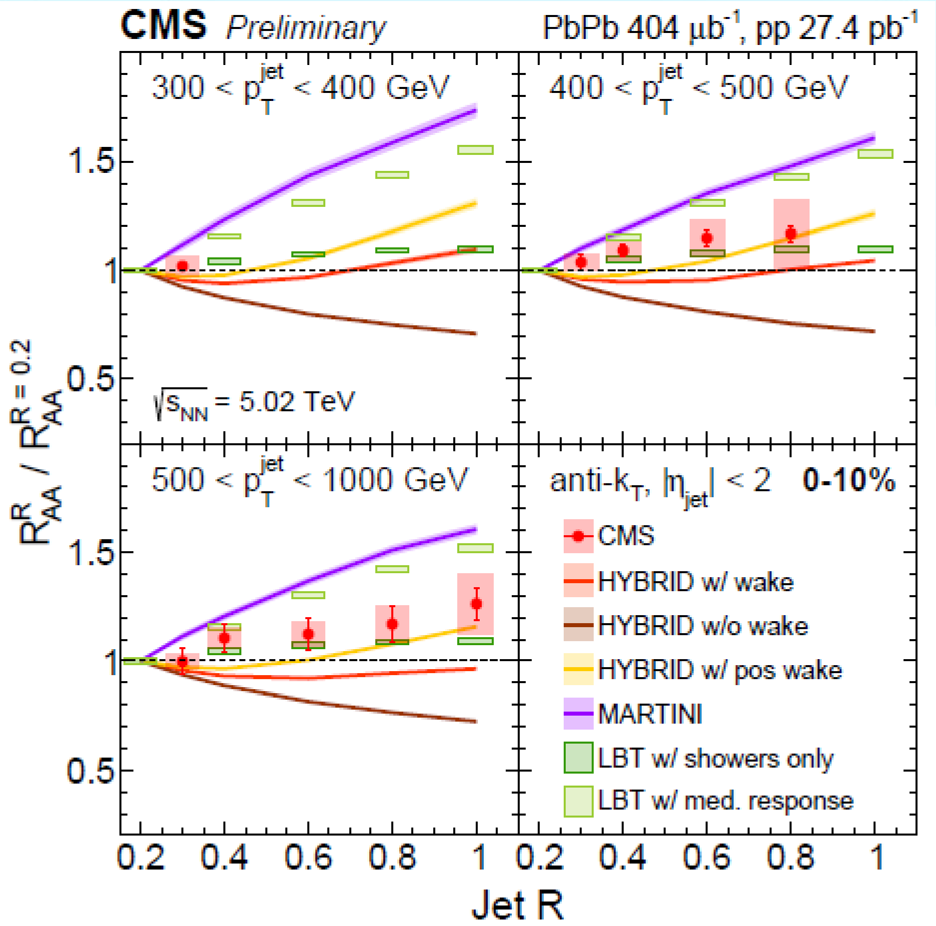

CMS Collaboration, JHEP 05 (2021) 284

Jet Observables in HIC

Jet anisotropic flow

$$\frac{dN}{d\phi} = C[1 + 2v_n \cos(n(\phi - \Psi_n))]$$

- ❖ $n = 1$ direct flow
- ❖ $n = 2$ elliptic flow
- ❖ $n = 3$ triangle flow
- ❖ …

For elliptic flow

- ✓ Strong centrality dependence – initial geometry and jet quenching
- ✓ Weak p_T and colliding energy dependence – competition btw the initial spectrum and jet quenching
- ✓ Potential to understand the path length dependence of jet quenching

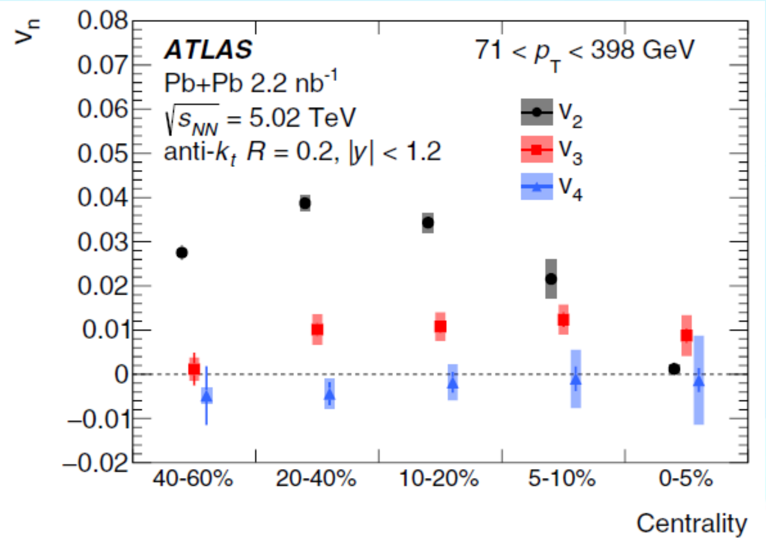

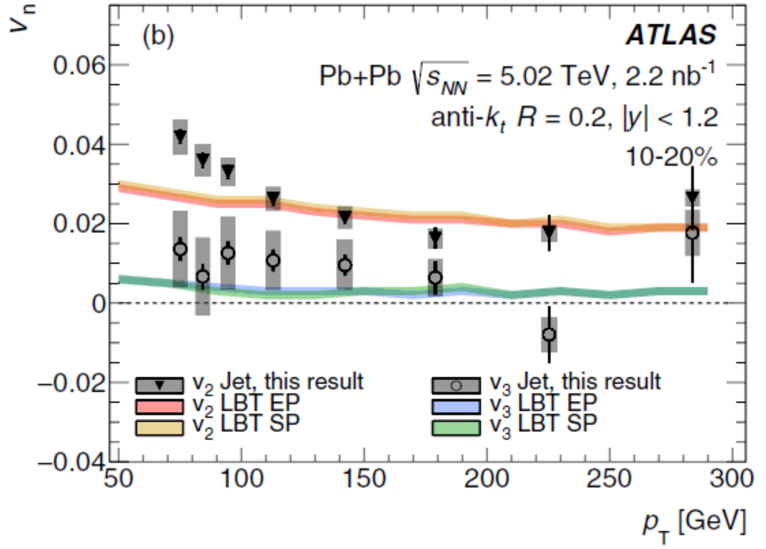

ATLAS Collaboration, PRC 105, 064903 (2022)

Jet Observables in HIC

Other jet observables:

- ✓ Jet shape, Jet fragmentation functions, Groomed jet mass and z_g
- ✓ Energy-energy correlators
- ✓ …

Questions to answer:

- 🤔 How jets are quenched, and how the energy in jets is distributed after jet quenching
- 🤔 How the QGP medium is modified due to energy deposition, and how the energy evolves

Jet Transport Model

Linear Boltzmann Transport (LBT) model

Code available at: “https://github.com/lbt-jet”

$$p_a \cdot \partial f_a = \frac{\gamma_b}{2}\int \Sigma_{bcd} \prod_{i=b,c,d} \frac{d^3 p_i}{2E_i(2\pi)^3}(f_c f_d - f_a f_b)|M_{ab\to cd}|S_2(\hat{s},\hat{t},\hat{u})(2\pi)^4\delta^4(p_a+p_b-p_c-p_d) + \text{inelastic}$$

$$S_2(\hat{s},\hat{t},\hat{u}) = \theta(\hat{s} > 2\mu_D^2)\theta(-\hat{s}+\mu_D^2 \le \hat{t} \le -\mu_D^2),$$

$$\mu_D^2 = \frac{3}{2}g^2T^2$$

Braaten and Pisarski, PRL 64 (1990) 1338

- Elastic: $\Gamma_a^{el} = \frac{p\cdot u}{p_0}\Sigma_{bcd}\,\rho_b(x)\sigma_{ab\to cd}$

LO pQCD

J. Auvinen et al, PRC 82(2010) 024906

- Inelastic: $\frac{d\Gamma_a^{inel}}{dz dk_\perp^2} = \frac{6\alpha_s P_a(z) k_\perp^4}{\pi\left(k_\perp^2+z^2m^2\right)^4}\cdot\frac{p\cdot u}{p_0}\hat{q}_a \sin^2\left(\frac{\tau-\tau_i}{2\tau_f}\right)$

High twist

Guo and Wang, PRL 85 (2000) 3591

Zhang, Wang and Wang, PRL 93 (2004) 072301

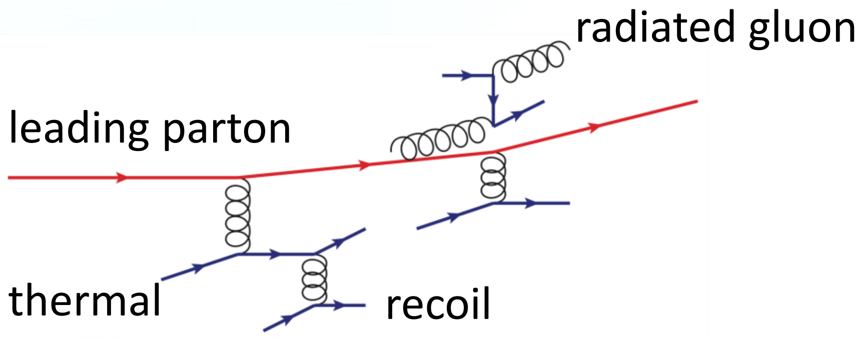

“negative”

- Multiple scattering
- Medium response: recoil – negative
- Linear approximation

Jet Transport Model

Coupled hydro + Linear Boltzmann Transport model（CoLBT）

Hard

Initial shower partons
(PYTHIA, SHERPA …)

Hard scattering (LBT)
$p_1 \cdot \partial f(x_1, p_1) = E_1 \quad (\mathcal{C}_{el} + \mathcal{C}_{inel})$

Recombination
Fragmentation

Real-time feedback
(local temperature, velocity …)

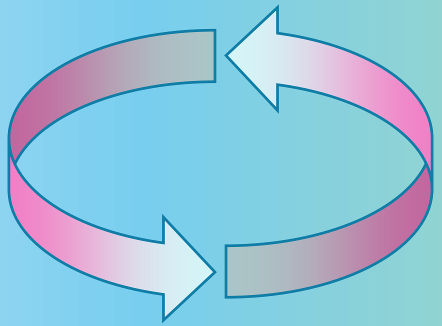

$j^{\nu} = \Sigma_i^n \frac{\mathrm{dp}_i^{\nu}}{d\tau} \delta^3(\vec{x} - \vec{x}_i)\theta(p_{cut}^0 - p_i \cdot u)$

Hadronization

Jet reconstruction

Soft

Initial condition
(AMPT, TRENTO)

QGP evolution (CLVisc)
$\partial_\mu T^{\mu\nu} = j^{\nu}$

Cooper-Frye

Fig. courtesy：
Tan Luo, QM 2019

Energy Loss

Path length dependence: $\hat{q}_a \approx C_2(a)\frac{42\,\xi(3)}{\pi}\ln\frac{2.6\,ET}{4\mu_D^2}$

- ➢ Elastic： linear dependence on path length — *He, Luo, Wang & Zhu, PRC 91, 054908 (2015)*
- ➢ Inelastic: quadratic at the early stage — *Luo, He, Cao & Wang, PRC 109, 034919 (2024)*
- ➢ Energy transfers from the hard to the soft

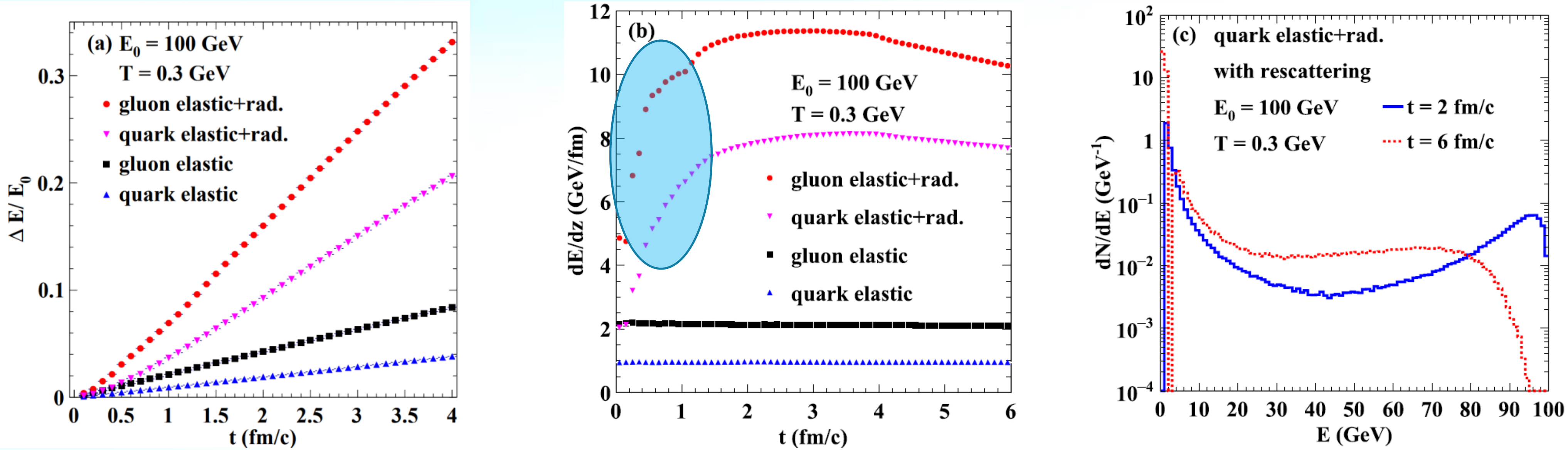

Bayesian Analysis of Energy loss

Jet energy loss distributions

He, Pang & Wang, PRL 122, 252302 (2019)

$$\frac{d\sigma_{AA}^{\text{jet}}}{dp_T dy}(p_T, R) \approx N_{\text{bin}}(b) \int d\Delta p_T \, \frac{d\sigma_{pp}^{\text{jet}}}{dp_T dy}(p_T + \Delta p_T, R) \, W_{AA}(\Delta p_T, p_T + \Delta p_T, R)$$

MC transport models: $\left.\begin{matrix} \sigma_{pp}^{\text{jet}}(p_T) \\ W_{AA}(p_T, \Delta p_T) \end{matrix}\right\} \Longrightarrow \sigma_{AA}^{\text{jet}}(p_T)$

Bayesian analysis: $\left.\begin{matrix} \sigma_{pp}^{\text{jet}}(p_T) \\ \sigma_{AA}^{\text{jet}}(p_T) \end{matrix}\right\} \Longrightarrow W_{AA}(p_T, \Delta p_T)$

Data-driven & model-independent

$$P(X|Y) = \frac{P(Y|X)P(X)}{P(Y)}, Y: data, X: W_{AA}$$

Parametrization:

$$W_{AA}(x) = \frac{\alpha^\alpha x^{\alpha-1} e^{-\alpha x}}{\Gamma(\alpha)} \qquad x = \frac{\Delta p_T}{\langle \Delta p_T \rangle}$$

$$\langle \Delta p_T \rangle = \beta (p_T / p_{T,0})^\gamma \log(p_T / p_{T,0})$$

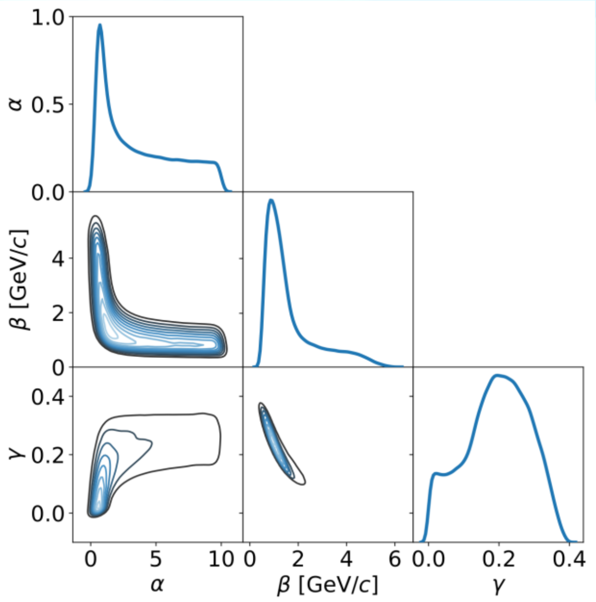

Posterior distributions

Bayesian Analysis of Energy loss

single inclusive jet in Pb+Pb			
	(0-10%)2.76 TeV	(20-30%)2.76 TeV	(0-10%)5.02 TeV
α	3.87 ± 2.93 (1.45 ± 0.01)	4.47 ± 2.83 (1.33 ± 0.02)	4.41 ± 2.86 (1.58 ± 0.02)
β	1.40 ± 1.12 (1.39 ± 0.06)	1.12 ± 0.47 (1.08 ± 0.07)	1.06 ± 0.97 (1.56 ± 0.06)
γ	0.21 ± 0.09 (0.21 ± 0.01)	0.15 ± 0.07 (0.20 ± 0.01)	0.26 ± 0.06 (0.23 ± 0.01)

γ-triggered jet in Pb+Pb			
	(0-30%)2.76 TeV	(30-100%)2.76 TeV	(0-30%)5.02 TeV
α	2.13 ± 1.28 (1.95 ± 0.12)	3.75 ± 2.81 (1.04 ± 0.06)	0.90 ± 0.09 (1.84 ± 0.13)
β	2.68 ± 1.40 (0.72 ± 0.06)	0.55 ± 0.44 (0.53 ± 0.04)	1.50 ± 0.85 (0.50 ± 0.04)
γ	0.16 ± 0.14 (0.44 ± 0.02)	0.13 ± 0.18 (0.30 ± 0.02)	0.21 ± 0.12 (0.56 ± 0.02)

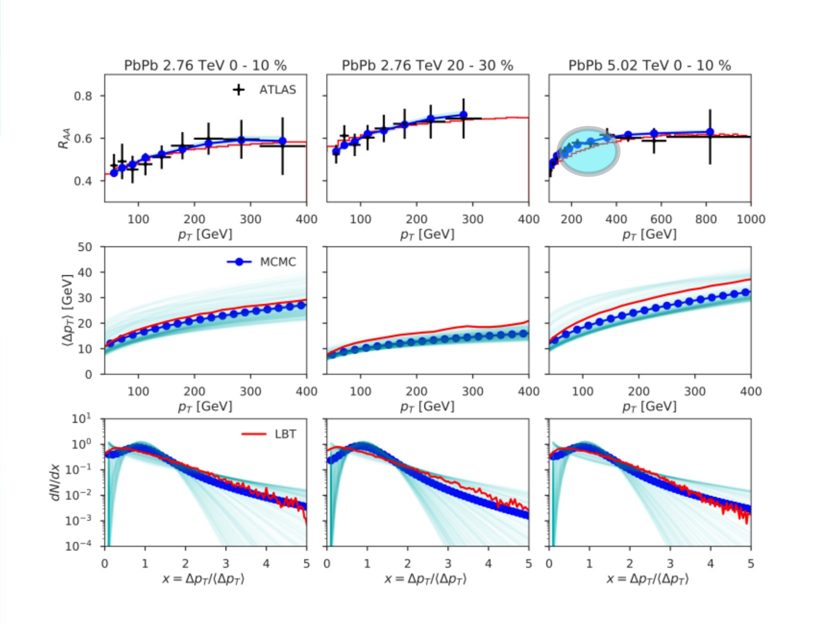

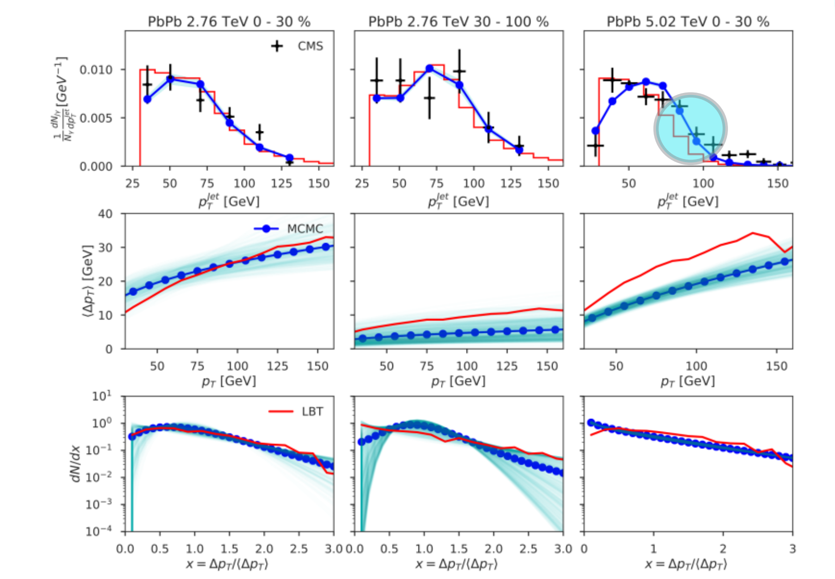

Transverse Momentum Broadening

$$\frac{d\Gamma_a^{inel}}{dzdk_\perp^2} = \frac{6\alpha_s P_a(z) k_\perp^4}{\pi(k_\perp^2 + z^2 m^2)^4} \cdot \frac{p \cdot u}{p_0} \hat{q}_a \sin^2\left(\frac{\tau - \tau_i}{2\tau_f}\right)$$

$$\hat{q}_a(x) = \sum_{bcd} \rho_b(x) \int d\hat{t}\, q_\perp^2 \frac{d\sigma_{ab\to cd}}{d\hat{t}} = \frac{\langle q_\perp^2 \rangle}{\lambda}$$

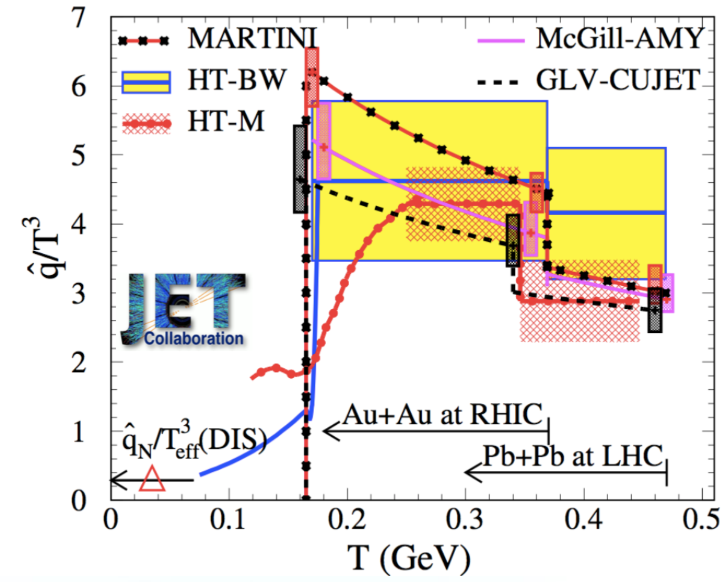

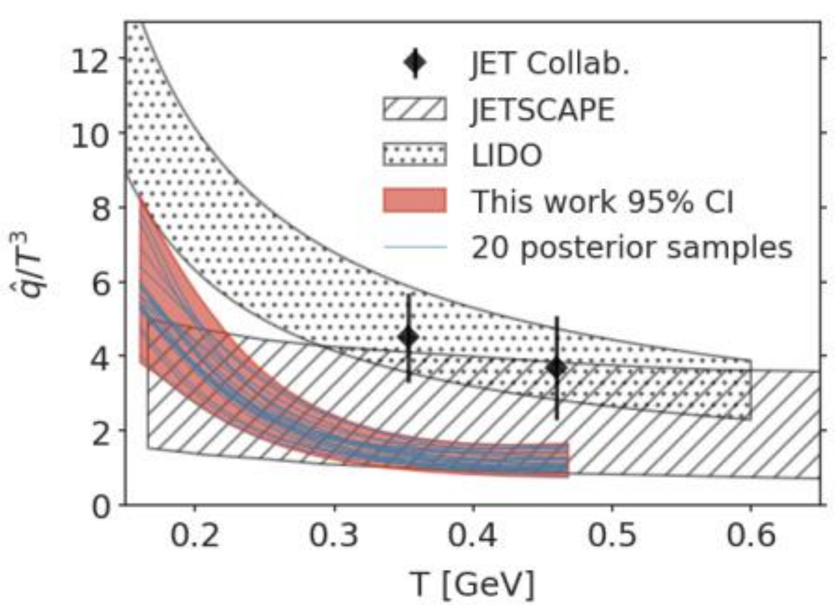

JET Collaboration, PRC 90, 014909 (2014)

JETSCAPE Collaboration, PRC 104, 024905 (2021)

Ke and Wang, JHEP 05, 041 (2021)

Xie, Ke, Zhang, and Wang, PRC 108 (2023) 1 L011901

$$\hat{q} \approx \begin{cases} 1.2 \pm 0.3 \\ 1.9 \pm 0.7 \end{cases} \mathrm{GeV}^2/\mathrm{fm} \text{ at } \begin{array}{l} \mathrm{T{=}370\ MeV} \\ \mathrm{T{=}470\ MeV} \end{array}$$

@RHIC
@LHC

Transverse Jet Tomography

Transverse jet tomography

He, Pang, and Wang, PRL 125 (2020) 122301

$$\frac{k^\mu}{\omega}\partial_\mu f_a(\vec{k},\vec{r}) = \frac{\hat{q}_a}{4}\vec{\nabla}^2_{k_\perp} f_a(\vec{k},\vec{r})$$

$$\hat{q}_a = \sum_{bcd}\prod_{i=b,c,d}\int \frac{d^3k_i}{2E_i(2\pi)^3} f_b(k_b)(\vec{k}_{a\perp}-\vec{k}_{c\perp})^2 \times |\mathcal{M}_{ab\to cd}|^2 \frac{\gamma_b}{2}(2\pi)^4\delta^4(k_a+k_b-k_c-k_d)$$

If $\hat{q}_a = \text{constant}$ $\quad f_a(\vec{k},\vec{r},t) = 3\left(\frac{4\omega}{\hat{q}_a t^2}\right)^2 e^{-(\vec{r}_\perp - \frac{\vec{k}_\perp}{2\omega}t)^2 \frac{12\omega^2}{\hat{q}_a t^3} - \frac{k_\perp^2}{\hat{q}_a t}}$

diffusion $\sqrt{\langle k_\perp^2\rangle} = \sqrt{\hat{q}_a t}$ $\qquad \sqrt{\langle r_\perp^2\rangle} = t\sqrt{(\hat{q}_a t/3)/\omega}$

drift $\vec{r}_\perp = (\vec{k}_\perp/2\omega)t$

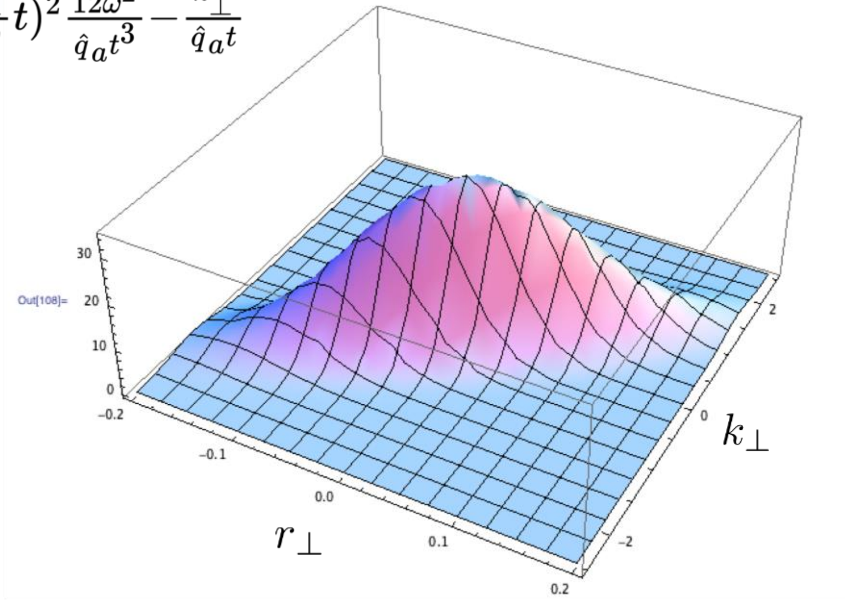

Transverse Jet Tomography

Transverse jet tomography

If $\hat{q} = \hat{q}_0 + \vec{a} \cdot \vec{r}_\perp$ $\qquad$ $f(\vec{k}_\perp, t) = [1 - \frac{t}{3\hat{q}_0 w} \vec{a} \cdot \vec{k}_\perp (1 - \frac{1}{2\hat{q}_0 t} \vec{k}_\perp^2)] f_s(\vec{k}_\perp, t)$

when $|\vec{a}|$ is small enough, the correction $\propto |\vec{a}|$

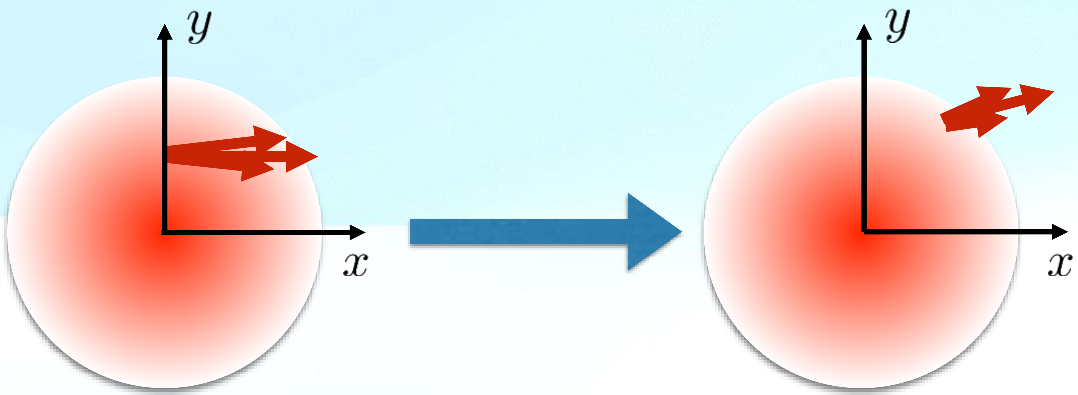

Distorted Gaussian

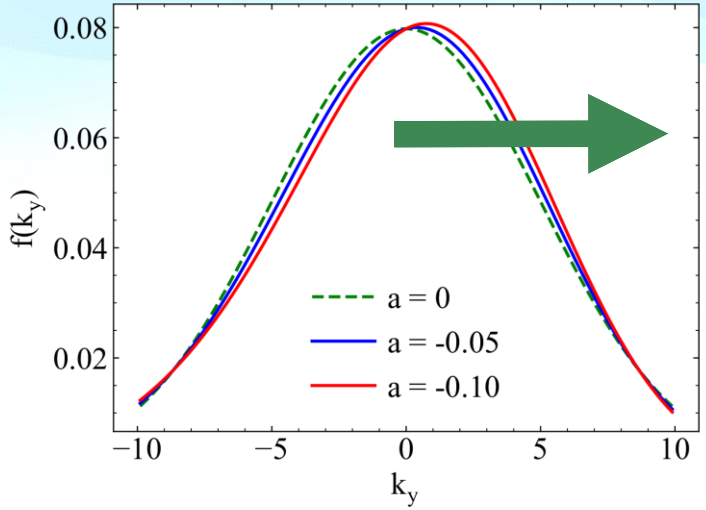

Jets tend to propagate to the lower $\hat{q}$ region

Transverse Jet Tomography

Simple model simulations

transverse number asymmetry:

$$A_N^y = \frac{f(k_y > 0) - f(k_y < 0)}{f(k_y > 0) + f(k_y < 0)}$$

similar to the QGP

$$\hat{q}(\vec{r}_\perp, t) = \frac{\hat{q}_0 t_0}{t_0 + t} e^{-x^2/a_x^2 - y^2/a_y^2}$$

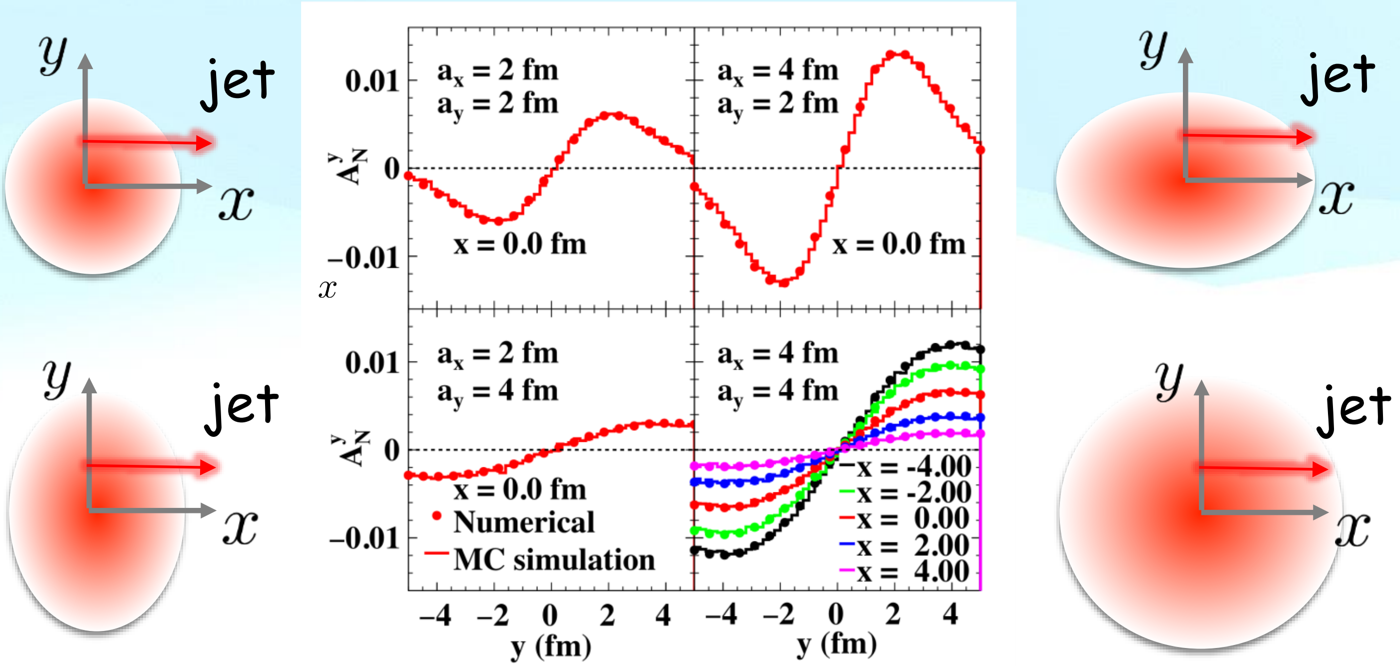

Larger gradient, and longer propagation give stronger transverse asymmetry

Gamma-jet Transverse Tomography

LBT model simulations

transverse energy asymmetry: $A^{y}_{E_T} = \dfrac{E_T(k_y > 0) - E_T(k_y < 0)}{E_T(k_y > 0) + E_T(k_y < 0)}$

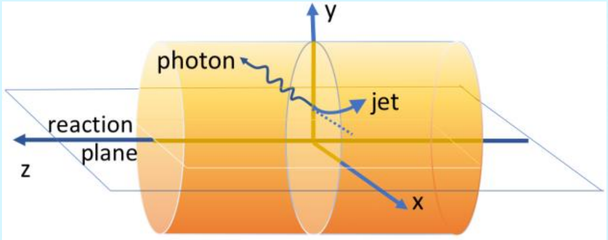

Jet tomography for jet localization

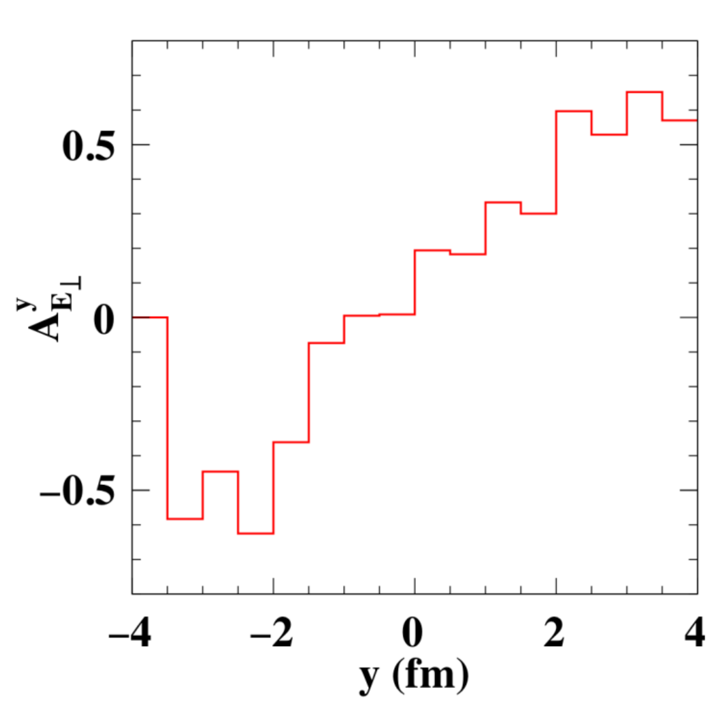

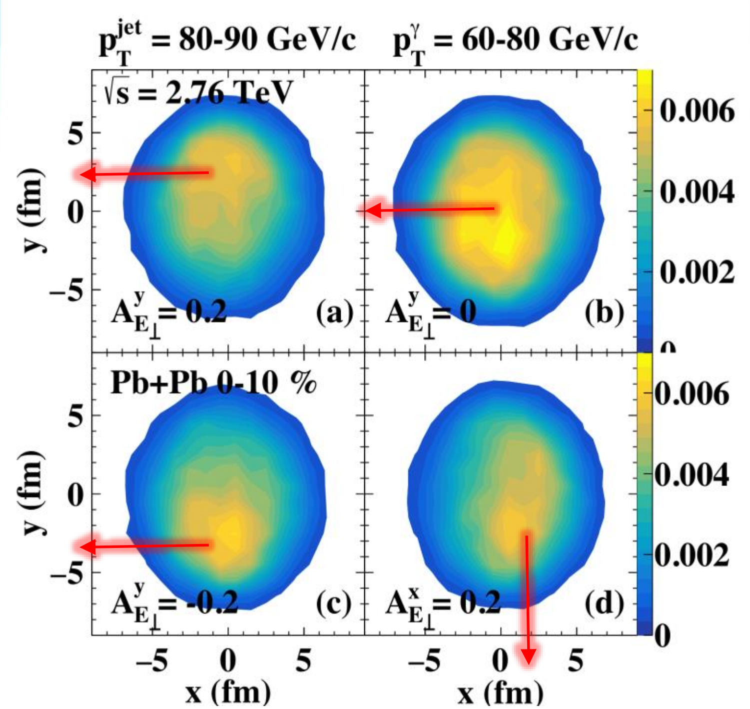

2D Dijet Tomography

Transverse jet tomography

He et al, in preparation

$$A_{E_T}^{y} = \frac{E_T(k_y > 0) - E_T(k_y < 0)}{E_T(k_y > 0) + E_T(k_y < 0)}$$

$500 < p_{T,1}^{AA} < 550\ \mathrm{GeV/c}$

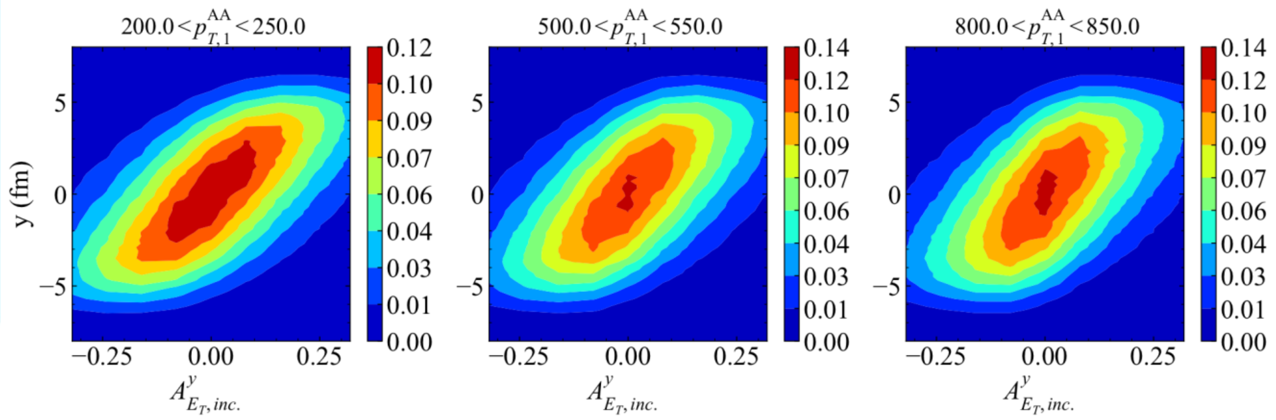

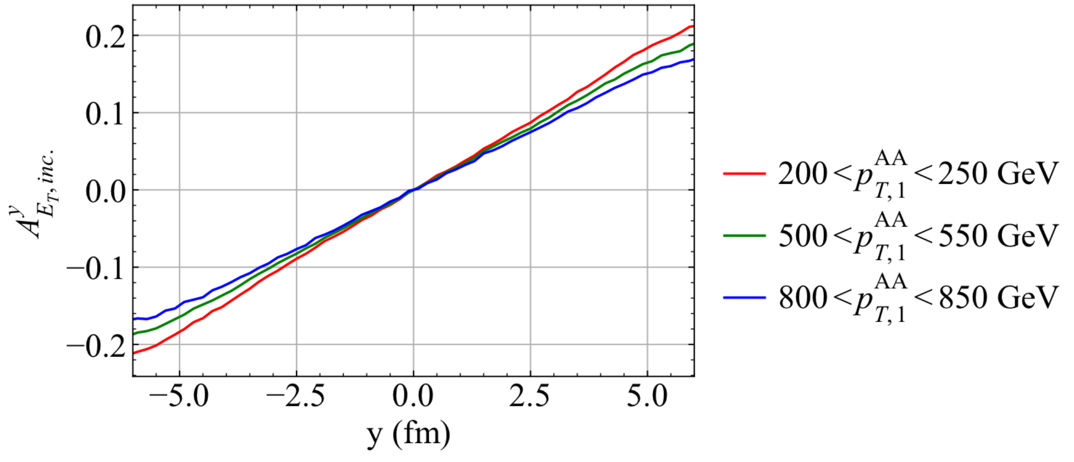

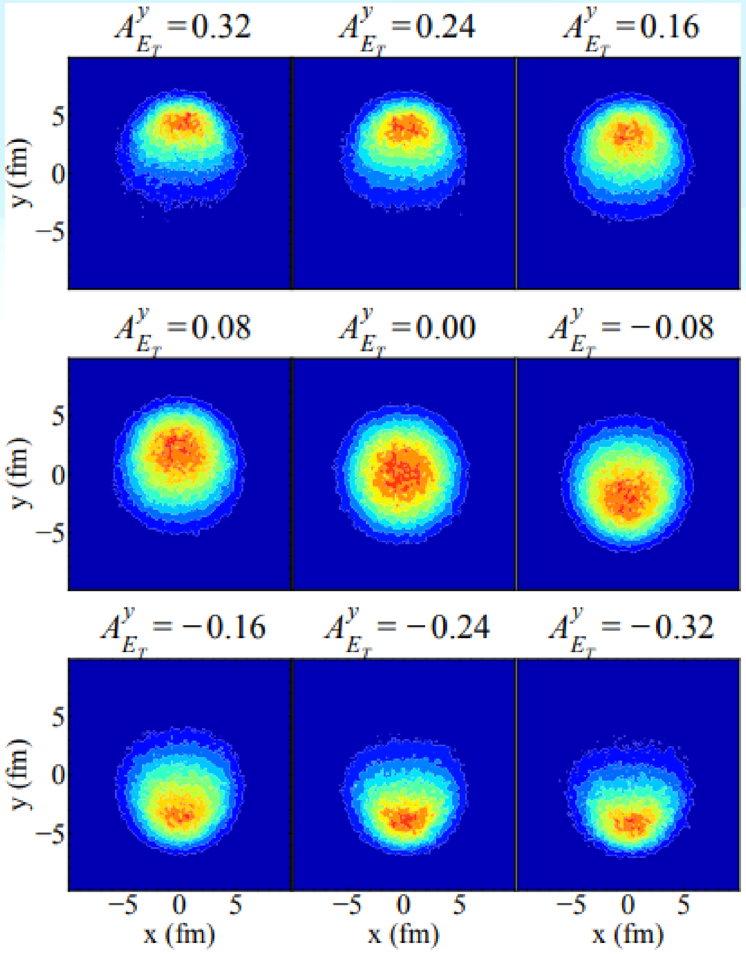

2D Dijet Tomography

Longitudinal jet tomography:

$$r_{e,2} = (p_{T,2}^{pp} - p_{T,2}^{AA})/p_{T,2}^{pp}$$

$500 < p_{T,1}^{AA} < 550$ GeV/c

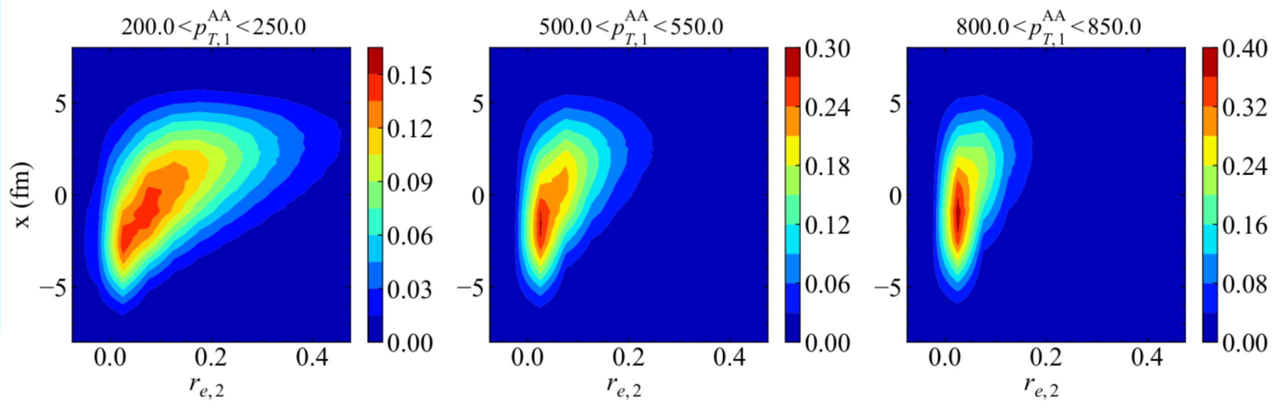

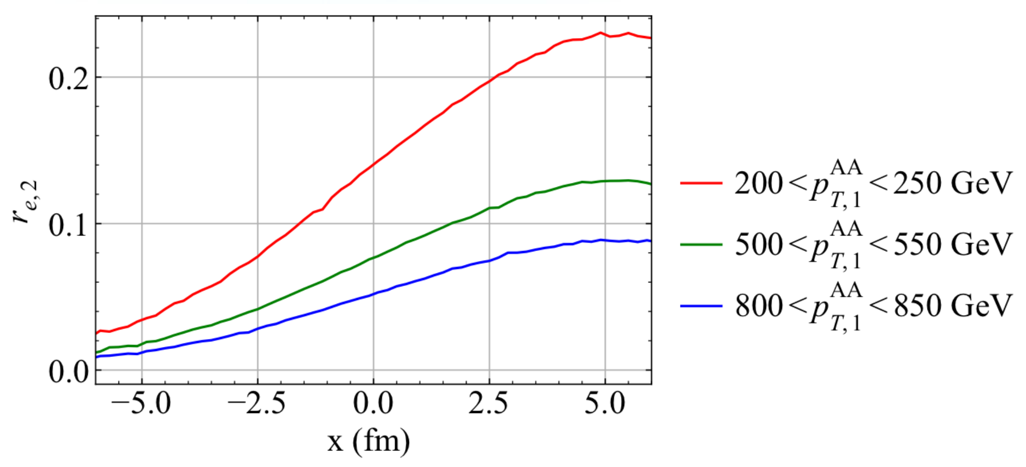

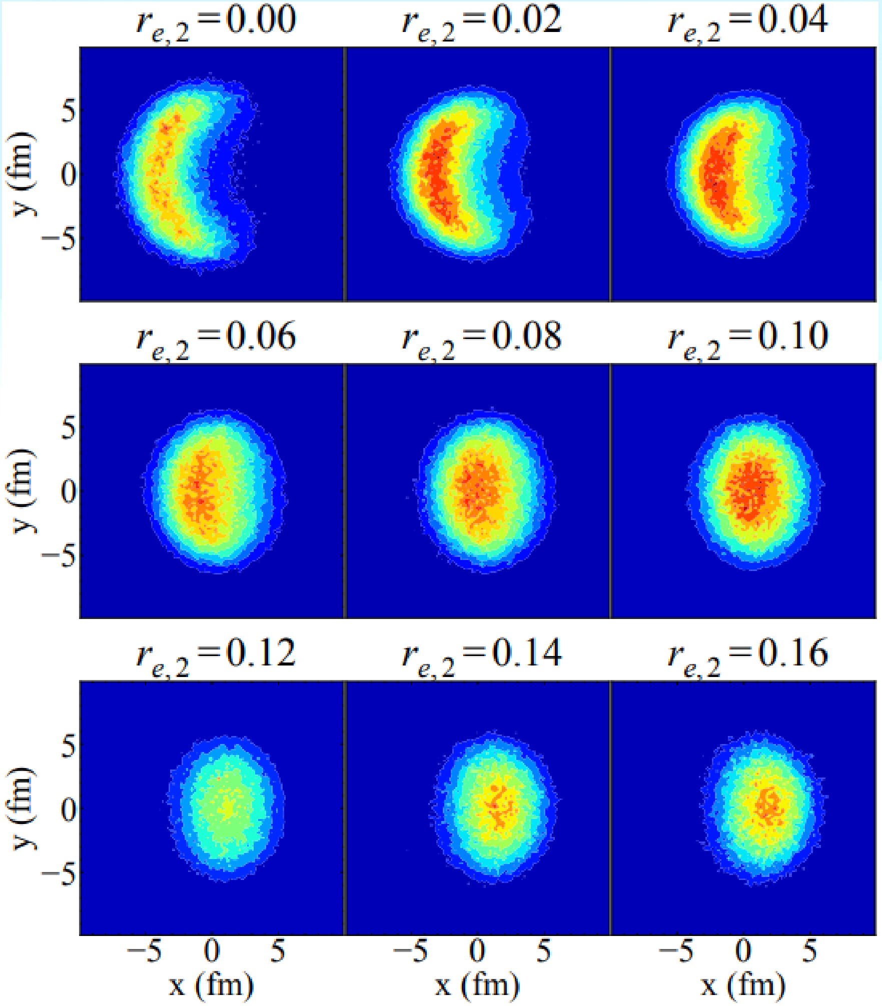

2D Dijet Tomography

$500 < p_{T,1}^{AA} < 550$ GeV/c

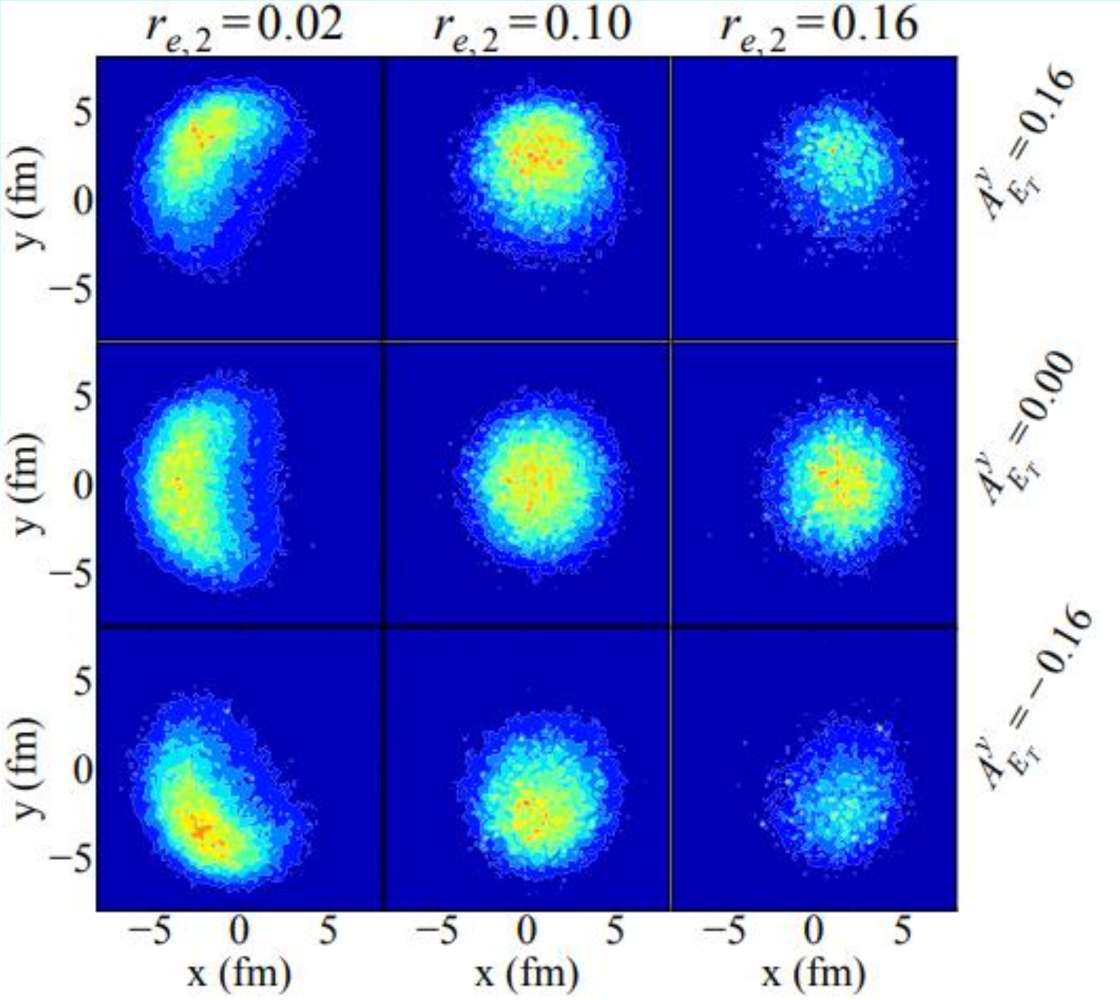

Transverse

+

longitudinal

jet tomography

Scan the QGP in the whole region!

Medium Response: recoil-negative

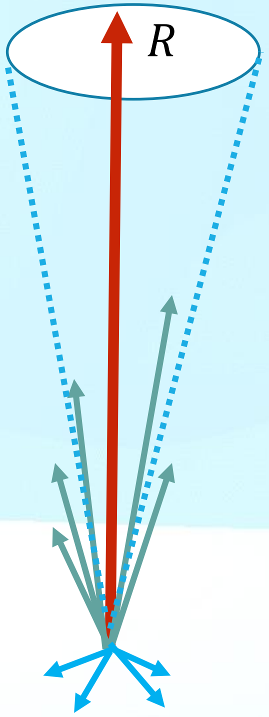

Jet parton, E

Recoil and
radiated gluon, w

"negative" parton,
particle hole, T

$E > w > T$

Diffusion wake: negative net contribution from medium response

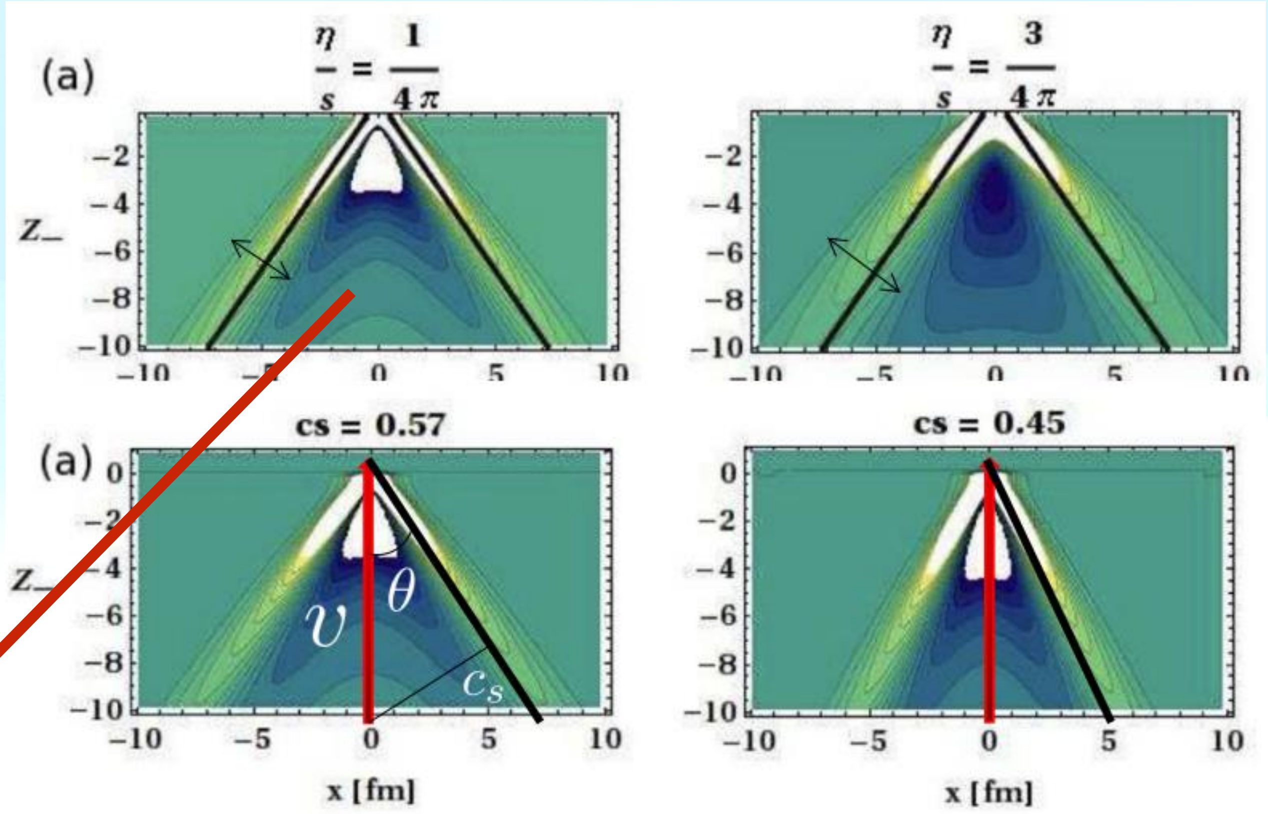

Neufeld. PRC 79 (2009) 054909

Width of front wake is related to the shear viscosity, $D^2 \sim \frac{\eta}{sT}$

Angle of mach cone is related to the speed of sound, $\sin(\theta) = \frac{c_s}{v}$

Medium Response: recoil-negative

Mach-cone-like structure

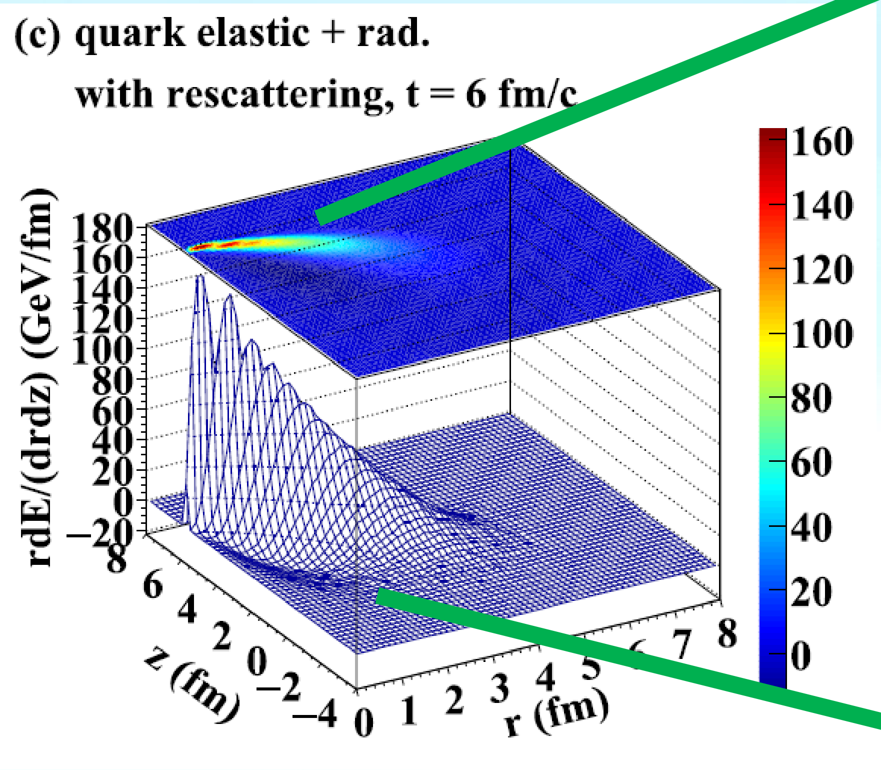

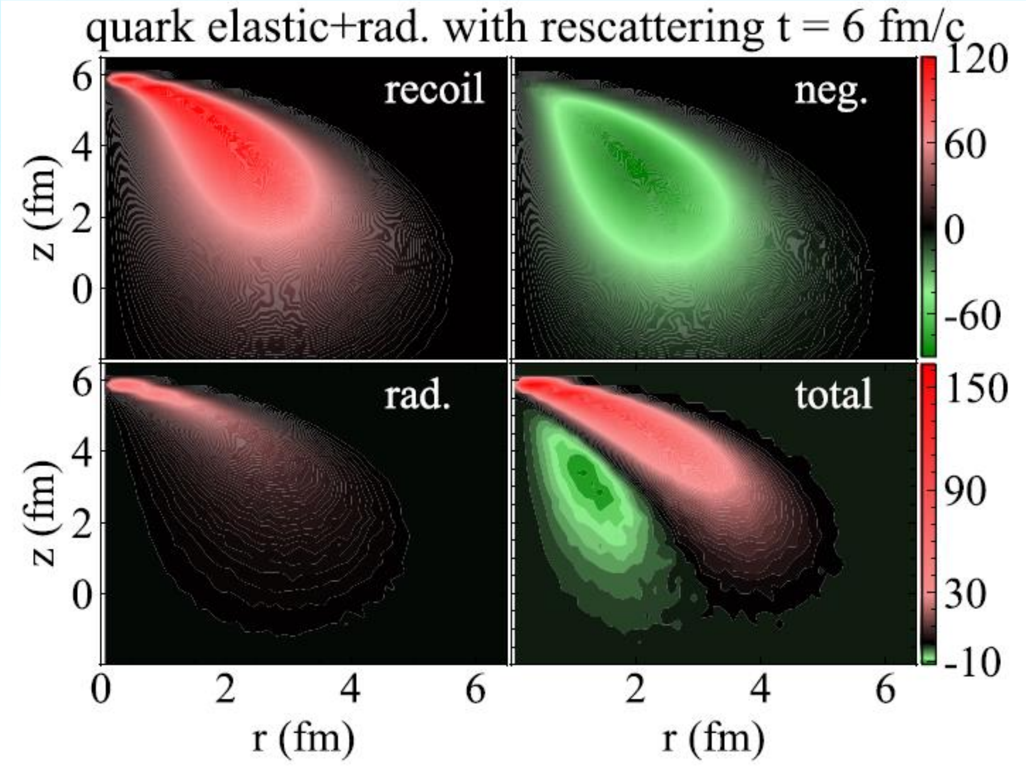

Diffusion wake

Medium Response: diffusion wake

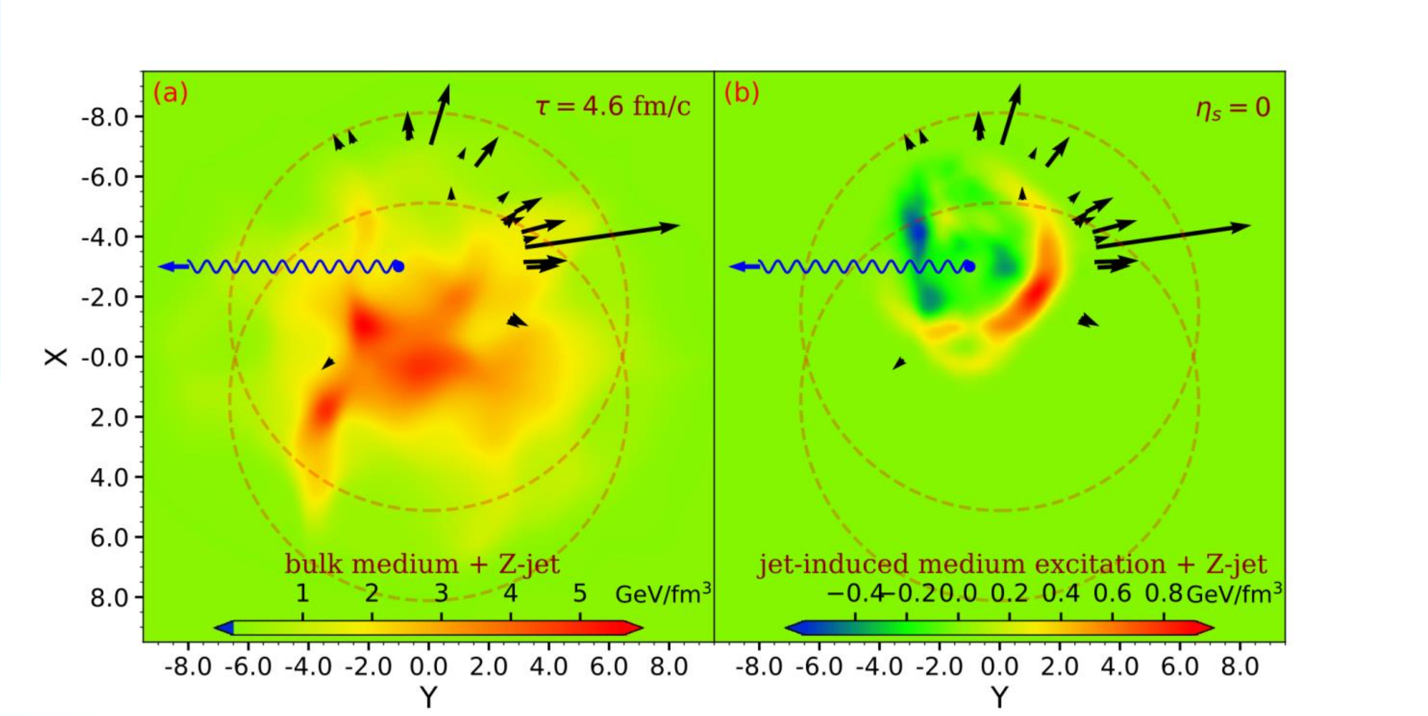

Medium Response: diffusion wake

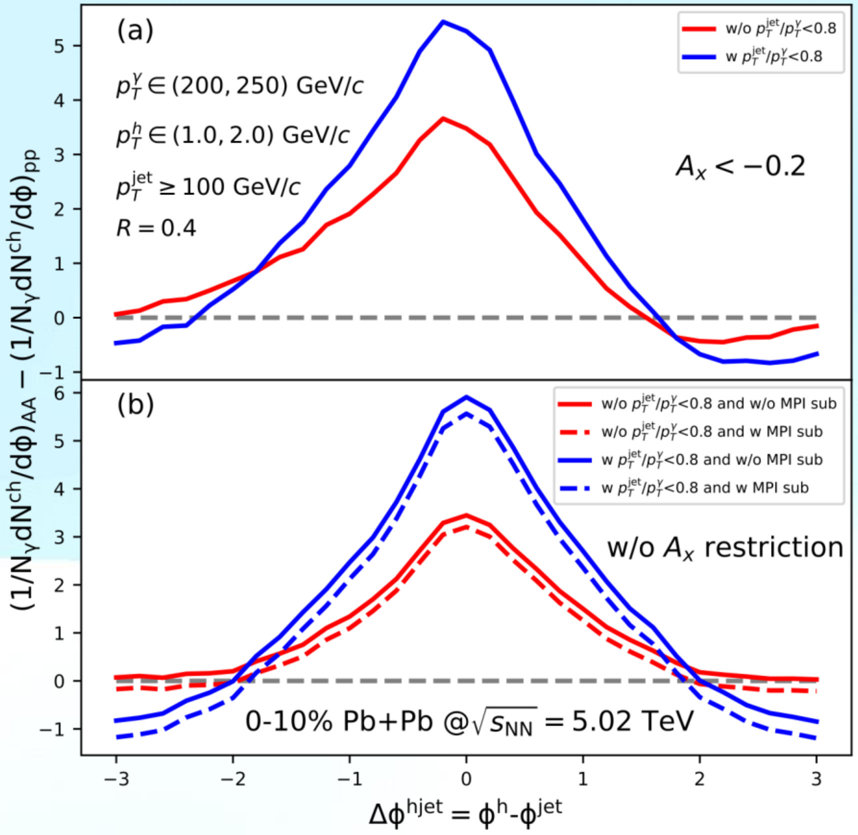

Chen, Yang, He, Ke, Pang, and Wang, PRL 127, 082301 (2021)

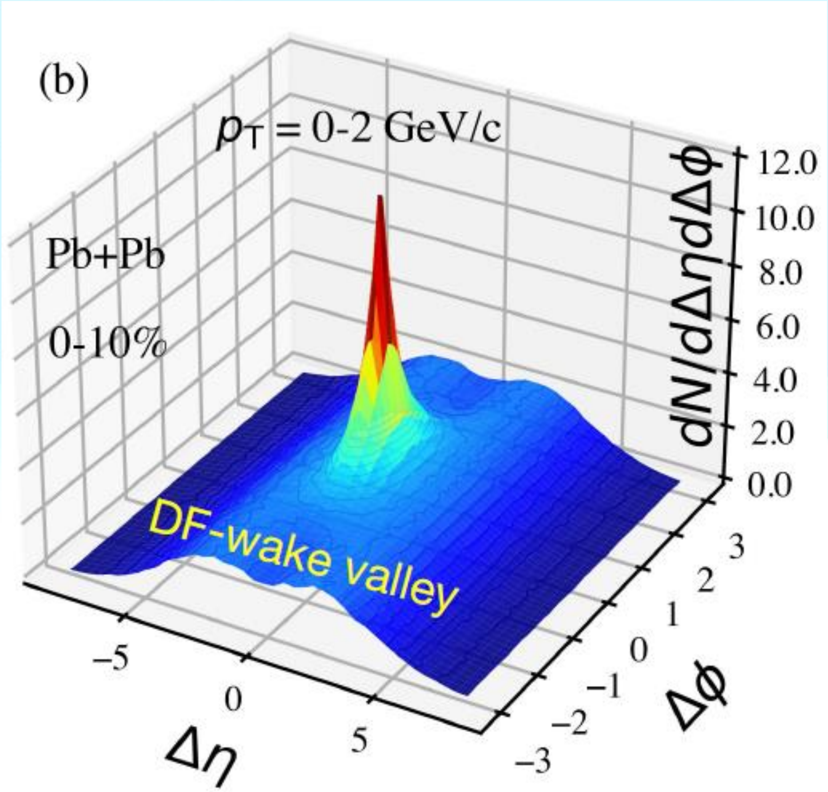

Yang, Luo, Chen, Pang, and Wang, PRL 130(5), 052301 (2023)

- ✓ 2D jet tomography can enhance the signal of diffusion wake
- ✓ 3D jet structure can be quenched to form diffusion wake in the longitudinal direction

Machine Learning Assisted

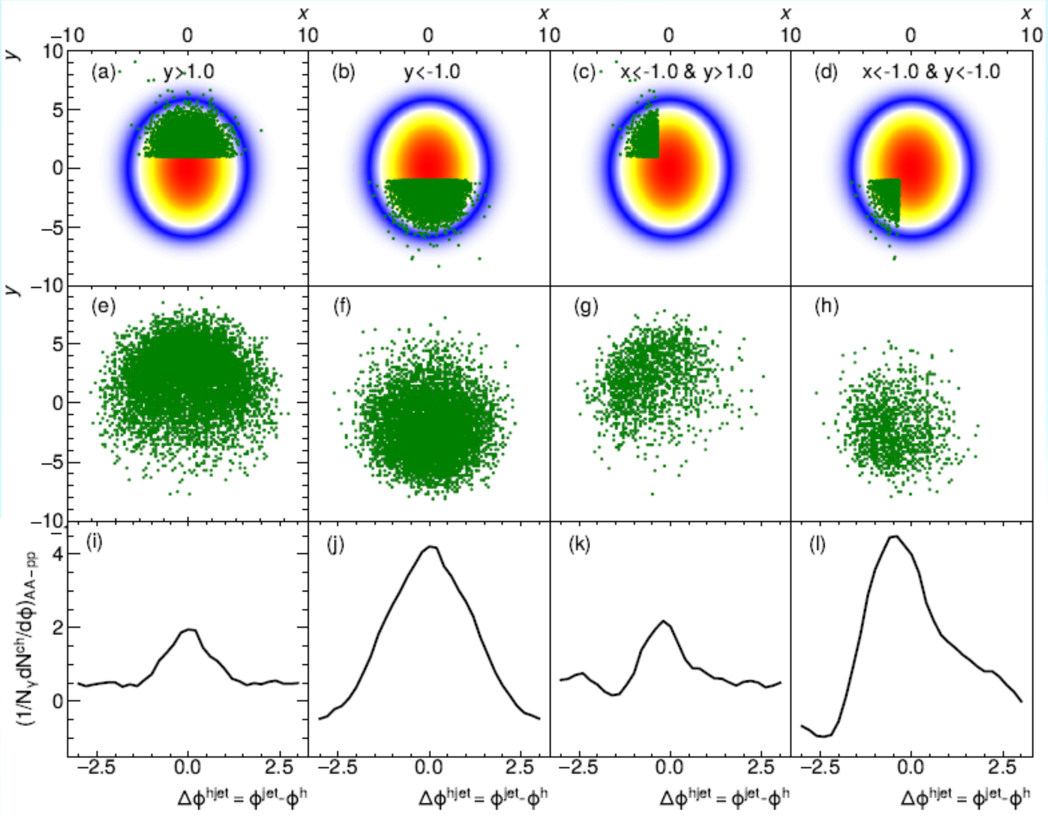

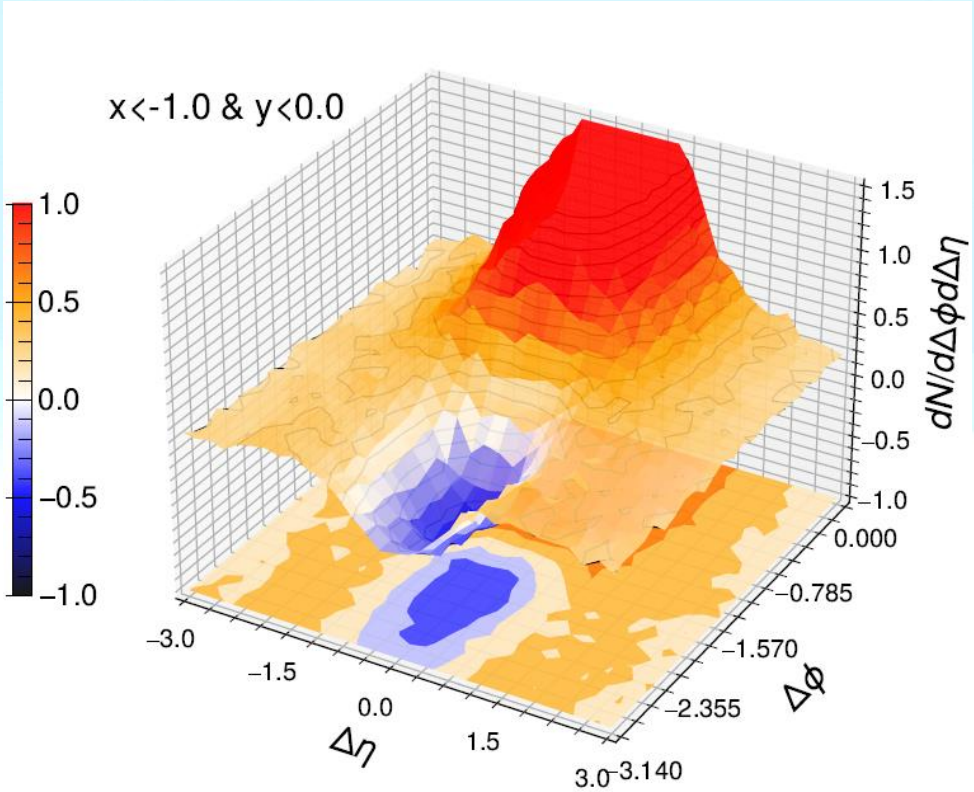

Yang, He, Chen, Ke, Pang, and Wang, EPJC (2023) 83:652

✓ Point Cloud NN to predict initial jet creation points, and search for diffusion wake

Energy-Energy Correlator

Definition and motivation

$$\frac{d\Sigma^n}{d\theta} = \frac{1}{\sigma}\Sigma_{i\neq j}\int d\vec{n}_{i,j}\,\frac{d\sigma_{i,j}}{d\vec{n}_{i,j}}\frac{E_i^n E_j^n}{Q^{2n}}\delta(\vec{n}_i\cdot\vec{n}_j - cos\theta)$$

1. IRC safe, pQCD calculable
2. Soft suppressed, easy to subtract background for experiments

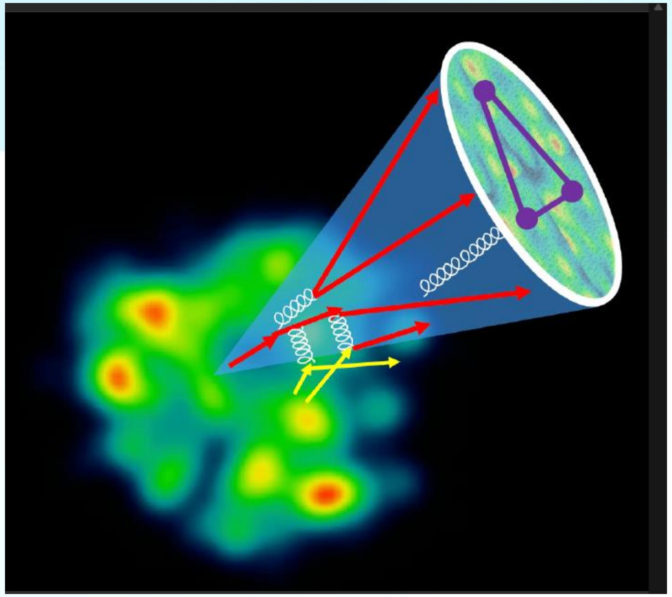

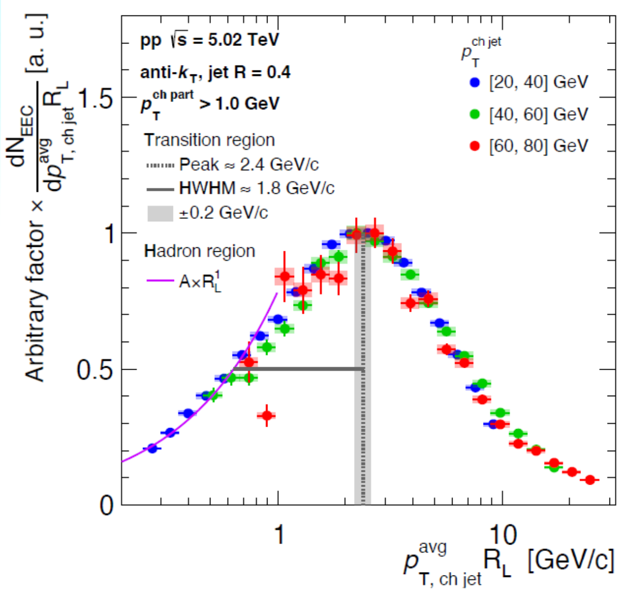

W. Fan, QM 2023

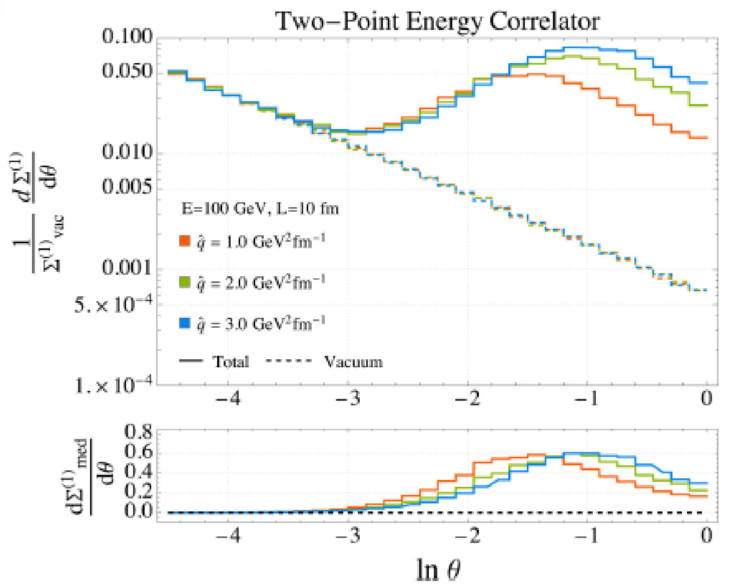

Ian Moult et al, PRL, 130, 262301 (2023)

EEC in vacuum

LO emission

$$\frac{d\Sigma_q^{vac}}{d\theta^2} \approx \frac{\alpha_s}{2\pi} C_F \int_0^1 dz\, z(1-z) P_{qg}(z) \int_{\mu^2}^{Q^2} \frac{dl_\perp^2}{l_\perp^2} \delta\left(\theta^2 - \frac{l_\perp^2}{[z(1-z)E]^2}\right)$$

$$\frac{d\Sigma_q^{vac}}{d\theta} \approx \frac{\alpha_s}{2\pi} \frac{C_F}{2\theta} \left(3 - \frac{2\mu}{E\theta}\right) \sqrt{1 - \frac{4\mu}{E\theta}}$$

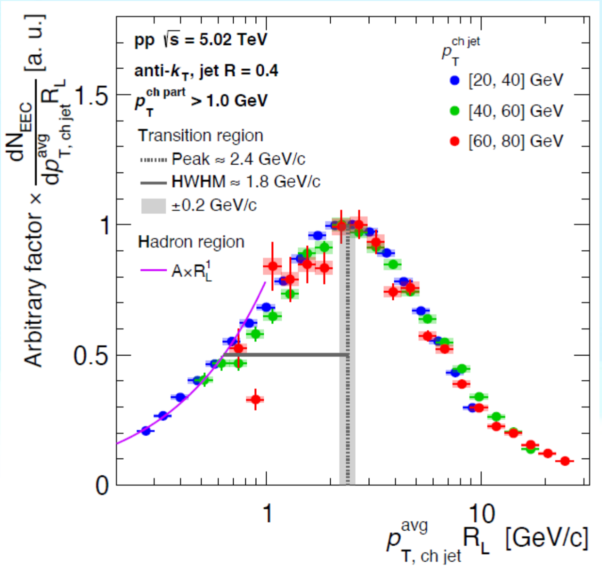

W. Fan, QM 2023

- **Large angle scaling**: $\frac{d\Sigma_q^{vac}}{d\theta} \sim \frac{1}{\theta}, \theta > \frac{4\mu}{E}$, perturbative, hard scattering
- **Transition angle region**: $\frac{d\Sigma_q^{vac}}{d\theta} \quad , \theta \to \frac{4\mu}{E}$, non-perturbative, hadronization
- **Small angles** : $\frac{d\Sigma_q^{vac}}{d\theta} \sim \theta, \theta < \frac{4\mu}{E}$, non-perturbative, hadronization

EEC in medium

High-twist induced emission in a QGP brick:

$$\frac{d\Sigma_q^{med}}{d\theta} \approx \frac{L^{\frac{5}{2}}\hat{q}}{\pi\sqrt{E}} \frac{8\alpha_s C_A}{\left(\sqrt{EL}\,\theta\right)^3} \int dz\, \frac{P_{qg}(z)}{z(1-z)}\left[1 - \frac{\sin ELz(1-z)\theta^2/8}{ELz(1-z)\theta^2/8}\right]$$

- Large angle scaling:

$$\frac{d\Sigma_q^{med}}{d\theta} \approx \frac{L^2\hat{q}}{2E}\frac{\alpha_s C_A}{\theta}$$

- Small angle scaling:

$$\frac{d\Sigma_q^{med}}{d\theta} \approx \frac{L^3\hat{q}}{64\pi}\alpha_s C_A \theta$$

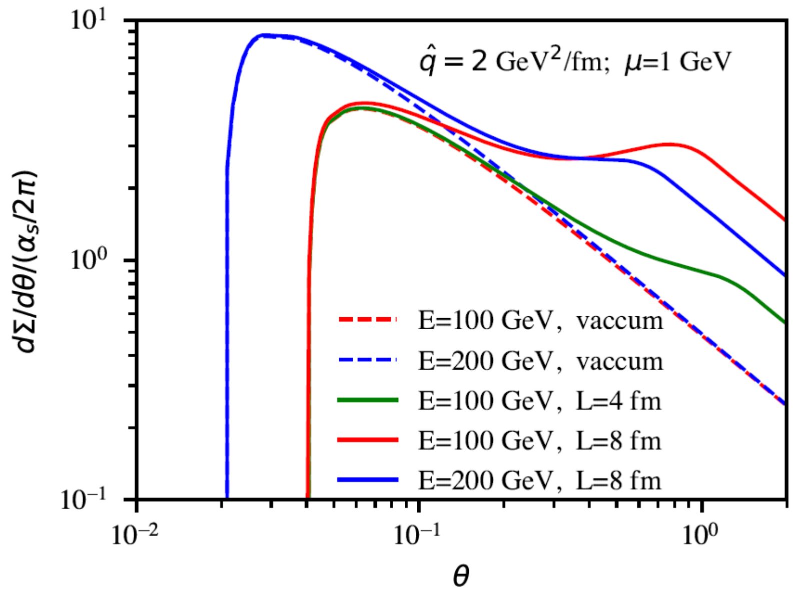

EEC to resolve QGP scales

Gluon emission in a QGP brick:

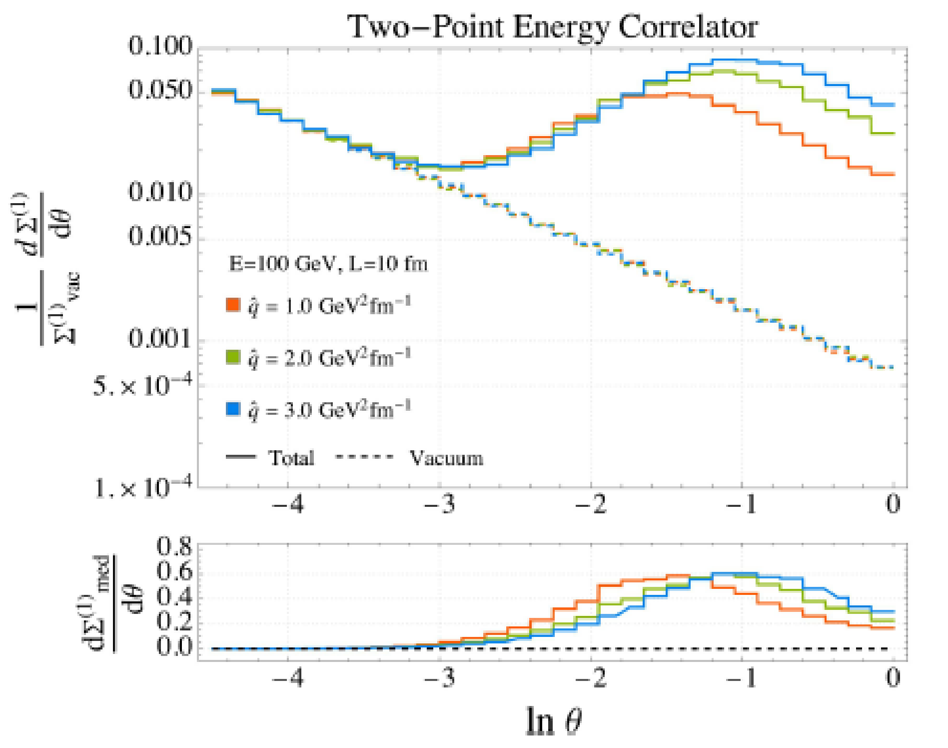

Ian Moult et al, PRL, 130, 262301 (2023)

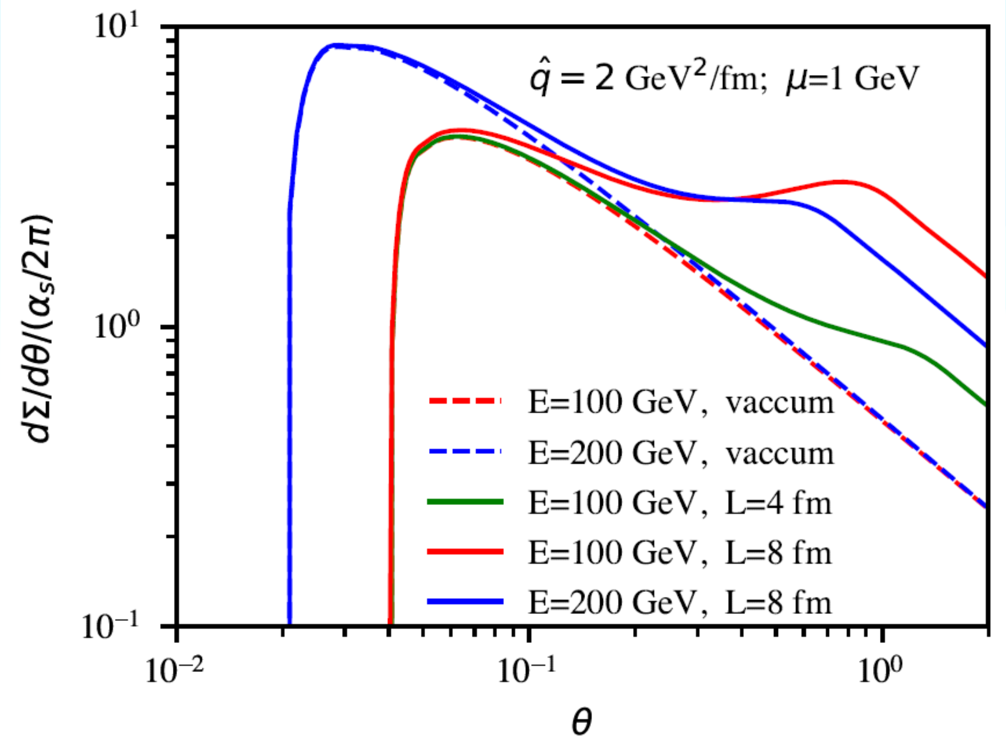

Yang, He, Moult & Wang, PRL 132, 011901 (2024)

EEC to resolve QGP scales

- Debye screen mass: $\mu_D^2 = \frac{3}{2} K g^2 T^2$, perturbative + nonperturbative
- Only vary *K* during the samplings of the transverse momentum transfer of $2 \rightarrow 2$ processes and kinematic limit

Single parton with multiple scatterings

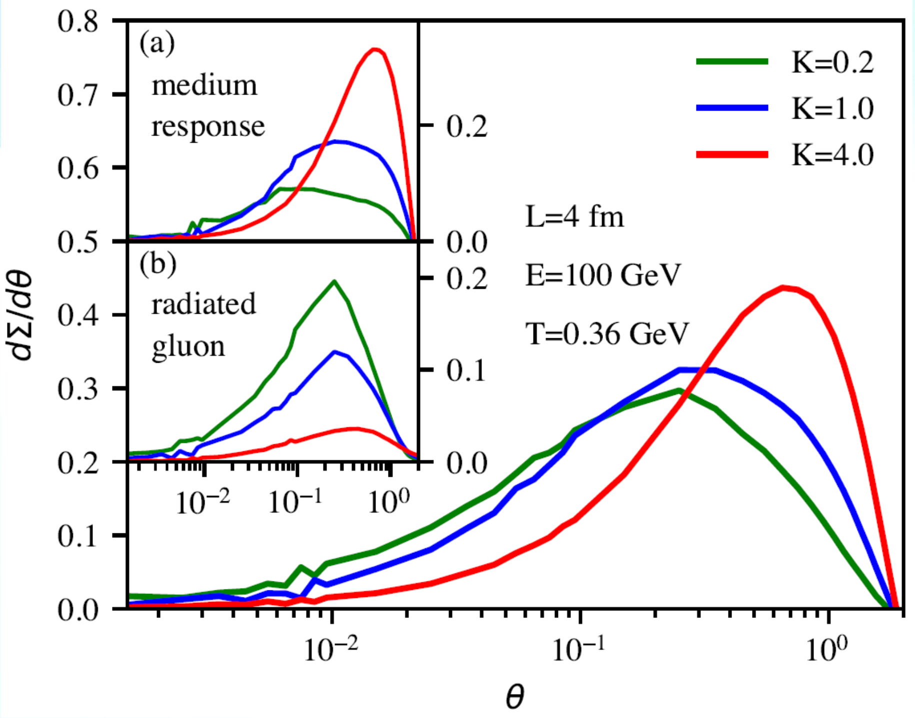

- ✓ Strong dependence on K, especially at large angles
- ✓ Medium response dominant
- ✓ Radiated gluon suppressed

EEC to resolve QGP scales

- Debye screen mass: $\mu_D^2 = \frac{3}{2} K g^2 T^2$, perturbative + non-perturbative
- Only vary K during the samplings of the transverse momentum transfer of $2 \to 2$ processes and kinematic limit

Shower partons with multiple scatterings

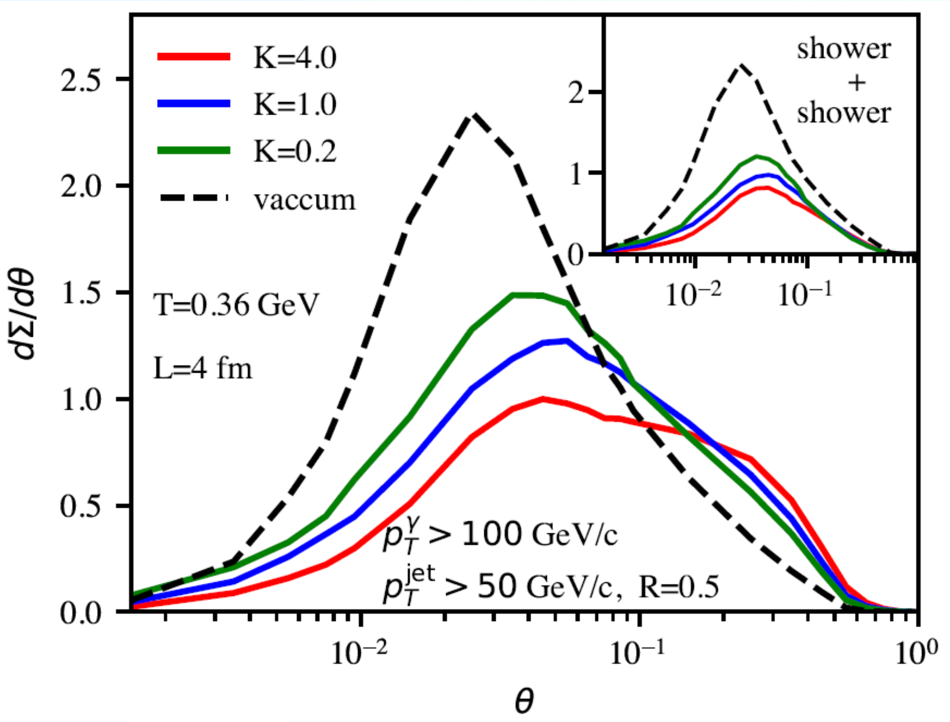

- ✓ Small angle suppressed due to energy loss and momentum broadening
- ✓ Large angle enhanced due to medium response and radiated gluons

EEC to resolve QGP scales

γ-jet in Pb+Pb 5.02 TeV 0-10 %

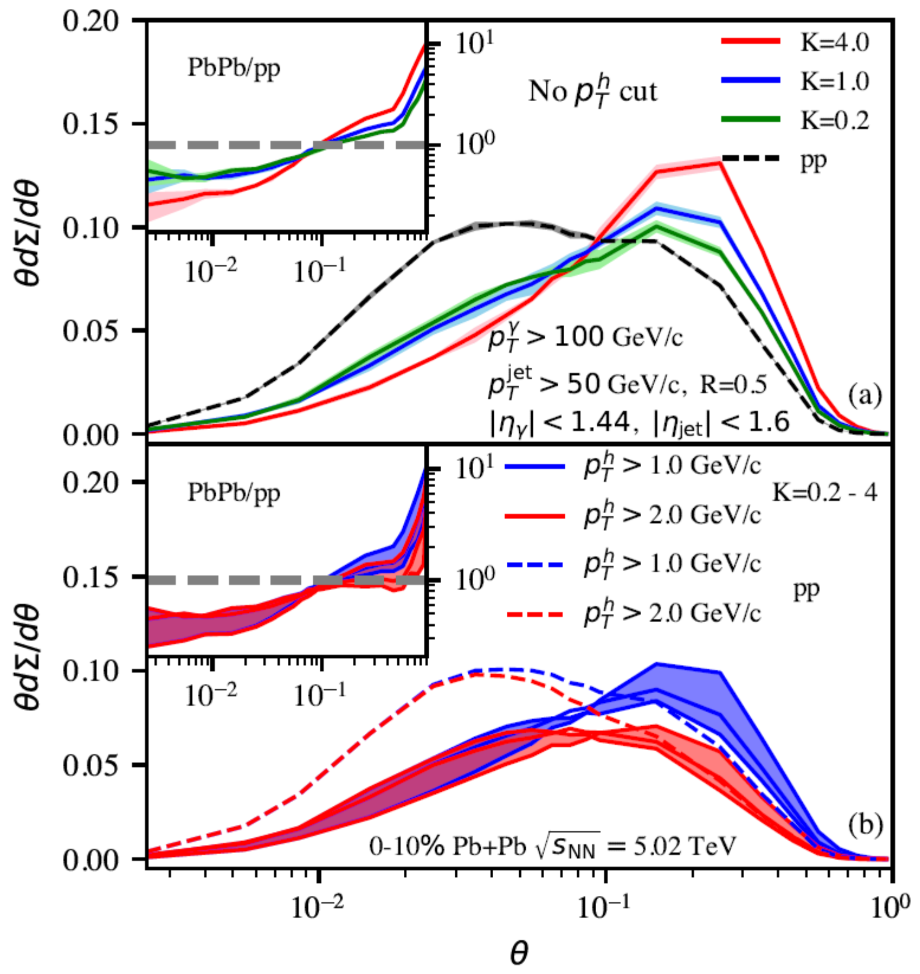

- ✓ Small angle suppressed due to energy loss and momentum broadening, insensitive to p_T cut
- ✓ Large angle enhanced due to medium response and radiated gluons, sensitive to p_T cut

Summary

- ✓ Jets are powerful probes to reveal QGP properties.
- ✓ Jet energy loss and the distributions can be extracted from experimental data with Bayesian analysis.
- ✓ Jet tomography can be used to localize initial jet production, and is promising to search for the diffusion wake.
- ✓ Energy-energy correlator is an excellent probe to investigate the short-distance structure of the QGP.

Thanks for your attention